

Multiple *N*-Methylation of MT-II Backbone Amide Bonds Leads to Melanocortin Receptor Subtype hMC1R Selectivity: Pharmacological and Conformational Studies

Lucas Doedens,^{†,‡} Florian Opperer,^{†,‡} Minying Cai,^{‡,§} Johannes G. Beck,^{†,‡} Matt Dedek,[§] Erin Palmer,[§] Victor J. Hruby,^{*,§} and Horst Kessler^{*,†}

Institute for Advanced Study and Center for Integrated Protein Science at the Technische Universität München, Lichtenbergstrasse 4, 85747 Garching, Germany, and Department of Chemistry and Biochemistry, University of Arizona, Tucson, Arizona, 85721

Received February 18, 2010; E-mail: kessler@ch.tum.de; hruby@email.arizona.edu

Abstract: Multiple *N*-methylation is a novel technology to improve bioavailability of peptides and increase receptor subtype selectivity. This technique has been applied here to the superpotent but nonselective cyclic peptide MT-II. A library of all possible 31 backbone *N*-methylated derivatives has been synthesized and tested for binding and activation at melanocortin receptor subtypes 1, 3, 4, and 5. It turned out that selectivity is improved with every introduced *N*-methyl group, resulting in several *N*-methylated selective and potent agonists for the hMC1R. The most potent of these derivatives is *N*-methylated on four out of five amide bonds in the cyclic structure. Its solution structure indicates a strongly preferred backbone conformation that resembles other α -MSH analogs but possesses much less flexibility and in addition distinct differences in the spatial arrangement of individual amino acid side chains.

Introduction

N-Methylation of peptide bonds is long known^{1–3} and has often been used to modify biological properties of bioactive peptides.⁴ However, it has become evident only recently that multiple *N*-methylation is a novel technology to improve the pharmacological properties of peptides⁵ and in extreme cases even achieve oral bioavailability⁶ such as found for the antibiotic Cyclosporin.^{7,8} Here we present a complete *N*-methylation library of the cyclic analogue of α -MSH, Ac-Nle-c[Asp-His-D-Phe-Arg-Trp-Lys]-NH₂ (MT-II), a biologically important and potent but nonselective agonist for the melanocortin receptor subtype family.^{9,10} The goal of our present study was to obtain new peptidic compounds with melanocortin receptor activity

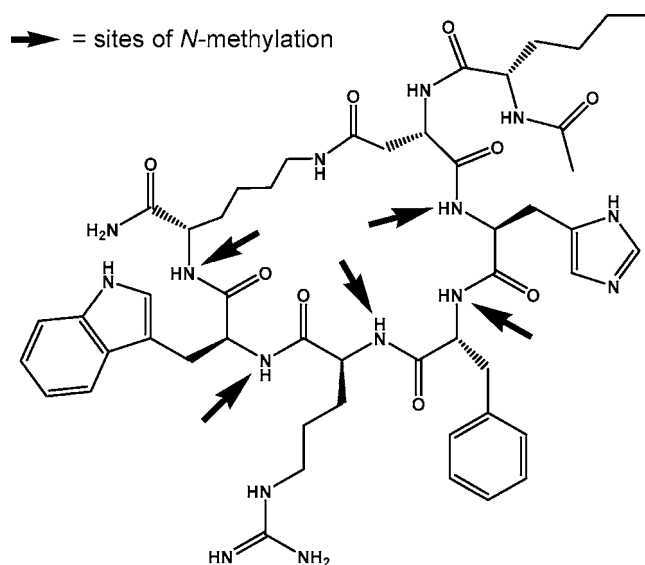


Figure 1. MT-II (Ac-Nle-cyclo(5 β →10 ϵ)(Asp⁵-His⁶-D-Phe⁷-Arg⁸-Trp⁹-Lys¹⁰)-NH₂) with sites of *N*-methylation indicated by arrows.

and improved selectivity, possessing pharmacological properties superior to those of MT-II. Therefore, we exchanged in a systematic manner His, D-Phe, Arg, Trp and Lys by their *N* ^{α} -methylated analogs and studied all of the 31 ($2^5 - 1 = 31$) possible MT-II-derivatives with one or more methylated backbone nitrogens (Figure 1).

The melanocortin receptors are members of the 7 transmembrane (TM) spanning G-protein coupled receptor (GPCR) superfamily. Five melanocortin receptor subtypes (MCR1–5)

[†] Institute for Advanced Study and Center for Integrated Protein Science at the Technische Universität München.

[‡] These authors contributed equally to this manuscript.

[§] University of Arizona.

- (1) Lindenberg, H. *J. Prakt. Chem.* **1875**, *12*, 244–259.
- (2) Fischer, E.; Bergmann, M. *Liebigs Ann. Chem.* **1913**, *398*, 96–124.
- (3) Fischer, E.; Lipschitz, W. *Ber. Dtsch. Chem. Ges.* **1915**, *48*, 360–378.
- (4) Gilon, C.; Dechantsreiter, M. A.; Burkhart, F.; Frieder, A.; Kessler, H. In *Houben-Weyl Methods of Organic Chemistry*; Georg Thieme Verlag: Stuttgart, 2003; Vol. E22c, pp 215–271.
- (5) Chatterjee, J.; Gilon, C.; Hoffman, A.; Kessler, H. *Acc. Chem. Res.* **2008**, *41*, 1331–1342.
- (6) Biron, E.; Chatterjee, J.; Ovidia, O.; Langenegger, D.; Brueggen, J.; Hoyer, D.; Schmid, H. A.; Jelinek, R.; Gilon, C.; Hoffman, A.; Kessler, H. *Angew. Chem., Int. Ed.* **2008**, *47*, 2595–2599.
- (7) Smith, J. M.; Hows, J. M.; Gordon-Smith, E. C. *J. Clin. Pathol.* **1983**, *36*, 41–43.
- (8) Sangalli, L.; Bortolotti, A.; Jiritano, L.; Bonati, M. *Drug. Metab. Dispos.* **1988**, *16*, 749–753.
- (9) Al-Obeidi, F.; Hadley, M. E.; Pettitt, B. M.; Hruby, V. J. *J. Am. Chem. Soc.* **1989**, *111*, 3413–3416.
- (10) Al-Obeidi, F.; Castrucci, A. M.; Hadley, M. E.; Hruby, V. J. *J. Med. Chem.* **1989**, *32*, 2555–2561.

have been discovered thus far.^{8,11–17} They all intracellularly mediate their effects by activating pathways that are cyclic adenosine monophosphate (cAMP) dependent. The diverse MCRs are distributed widely in mammalian tissues, and regulate numerous functions in the body including skin and hair coloration,^{18–20} inflammation²¹ and immunomodulation,²² steroid production and release,^{23,24} cardiovascular functions,^{25,26} energy homeostasis,²⁷ feeding behavior,^{28–30} penile erection and sexual behavior^{31–33} and many other functions. These very diverse biological activities generally are associated with only 1 or 2 of the melanocortin receptors that are expressed in different parts of the body. Thus, the search for highly selective and potent agonist and antagonist analogues is critical.

The natural endogenous agonistic ligands α -melanocyte stimulating hormone (α -MSH, Ac-Ser¹-Tyr²-Ser³-Met⁴-Glu⁵-His⁶-Phe⁷-Arg⁸-Trp⁹-Gly¹⁰-Lys¹¹-Pro¹²-Val¹³-NH₂), β -MSH, γ -MSH and adrenocorticotropin (ACTH) all are derived from the same precursor protein, pro-opiomelanocortin (POMC). Structure–function examinations of α -MSH and of α -MSH fragments have led to the identification of His-Phe-Arg-Trp as the critical pharmacophore for pigmentary activity and other functions of the melanotropin peptides.^{19,20,34–41} Truncation of the α -MSH sequence, keeping amino acids 4–10, exchange of

Met⁴ with Nle, Glu⁵ with Asp, Phe⁷ with D-Phe and Gly¹⁰ with Lys, acetylation of the Nle⁴- α -nitrogen, amidation of the C-terminal carboxyl function, and lactam cyclization resulted in the lactam bridged compound MT-II, a super potent but nonselective agonist at 4 melanocortin receptors MC1R, MC3R, MC4R, MC5R^{9,10,41} (not at the MC2R which has ACTH as its ligand, and where α -MSH and its analogues are not active).

A major focus in synthesizing new melanotropins is gaining selectivity and improved pharmacological properties that are suitable for medical applications of these compounds. When creating peptidic ligands, one possible way to obtain these properties is *N*-methylation of the amide bonds,^{4–6,42–44} since substitution of amide protons with methyl groups can result in receptor subtype selectivity,^{45–48} but also other pharmacological properties can be improved, such as metabolic stability^{6,49–51} lipophilicity,^{49–51} potency,^{52–55} bioavailability^{6,56,57} and con-

- (11) The Melanotropic Peptides. *Ann. N.Y. Acad. Sci.* **1993**, *680*, 1–687.
- (12) Chhajlani, V.; Wikberg, J. E. *FEBS Lett.* **1992**, *309*, 417–420.
- (13) Chhajlani, V.; Muceniece, R.; Wikberg, J. E. *Biochem. Biophys. Res. Commun.* **1993**, *195*, 866–873.
- (14) Gantz, I.; Konda, Y.; Tashiro, T.; Shimoto, Y.; Miwa, H.; Munzert, G.; Watson, S. J.; DelValle, J.; Yamada, T. *J. Biol. Chem.* **1993**, *268*, 8246–8250.
- (15) Gantz, I.; Miwa, H.; Konda, Y.; Shimoto, Y.; Tashiro, T.; Watson, S. J.; DelValle, J.; Yamada, T. *J. Biol. Chem.* **1993**, *268*, 15174–15179.
- (16) Gantz, I.; Shimoto, Y.; Konda, Y.; Miwa, H.; Dickinson, C. J.; Yamada, T. *Biochem. Biophys. Res. Commun.* **1994**, *200*, 1214–1220.
- (17) Labbe, O.; Desarnaud, F.; Eggerickx, D.; Vassart, G.; Parmentier, M. *Biochemistry* **1994**, *33*, 4543–4549.
- (18) The Melanocortin System. *Ann. N.Y. Acad. Sci.* **2003**, *994*, 1–367, provides the proceedings of a recent symposium discussing the latest developments in this area.
- (19) Hadley, M. E. in *The Melanotropin Peptides*; CRC Press: Boca Raton, FL, 1989.
- (20) Eberle, A. N. *The Melanotropins: Chemistry, Physiology and Mechanisms of Action*; Karger: Basel, 1988.
- (21) Manna, S. K.; Aggarwal, B. B. *J. Immunol.* **1998**, *161*, 2873–2880.
- (22) Maaser, C.; Kannengiesser, K.; Specht, C.; Luger, A.; Brzoska, T.; Luger, T. A.; Domschke, W.; Kucharzik, T. *Gut* **2006**, *55*, 1415–1422.
- (23) Xia, Y.; Wikberg, J. E. *Cell Tissue Res.* **1996**, *286*, 63–68.
- (24) Buckley, D. I.; Ramachandran, J. *Proc. Natl. Acad. Sci. U.S.A.* **1981**, *78*, 7431–7435.
- (25) Low, M. J. *J. Endocrinol. Invest.* **2004**, *27*, 95–100.
- (26) Li, S. J.; Varga, K.; Archer, P.; Hruby, V. J.; Sharma, S. D.; Kesterson, R. A.; Cone, R. D.; Kunos, G. *J. Neurosci.* **1996**, *16*, 5182–5188.
- (27) Gantz, I.; Fong, T. M. *Am. J. Physiol. Endocrinol. Metab.* **2003**, *284*, E468–474.
- (28) Fan, W.; Boston, B. A.; Kesterson, R. A.; Hruby, V. J.; Cone, R. D. *Nature* **1997**, *385*, 165–168.
- (29) Farooqi, I. S.; Keogh, J. M.; Yeo, G. S.; Lank, E. J.; Cheetham, T.; O’Rahilly, S. *N. Engl. J. Med.* **2003**, *348*, 1085–1095.
- (30) Branson, R.; Potoczna, N.; Kral, J. G.; Lentjes, K. U.; Hoehe, M. R.; Horber, F. F. *N. Engl. J. Med.* **2003**, *348*, 1096–1103.
- (31) Wessells, H.; Gralnek, D.; Dorr, R.; Hruby, V. J.; Hadley, M. E.; Levine, N. *Urology* **2000**, *56*, 641–646.
- (32) Wessells, H.; Levine, N.; Hadley, M. E.; Dorr, R.; Hruby, V. *Int. J. Impot. Res.* **2000**, *12* (4), S74–79.
- (33) King, S. H.; Mayorov, A. V.; Balse-Srinivasan, P.; Hruby, V. J.; Vanderah, T. W.; Wessells, H. *Curr. Top. Med. Chem.* **2007**, *7*, 1098–1106.
- (34) Eberle, A.; Hübscher, W. *Helv. Chim. Acta* **1979**, *62*, 2460–2483.
- (35) Eberle, A.; Schwyzler, R. *Helv. Chim. Acta* **1979**, *62*, 2452–2459.
- (36) Medzihradzsky, K. *Recent Developments in the Chemistry of Natural Carbon Compounds*; Hungarian Academy of Science: Budapest, 1976; pp 207–250.
- (37) Schwyzler, R.; Eberle, A. *Frontiers of Hormone Research*; Karger: Basel, 1977; Vol. 4, pp 18–25.
- (38) Hruby, V. J.; Wilkes, B. C.; Hadley, M. E.; Al-Obeidi, F.; Sawyer, T. K.; Staples, D. J.; de Vaux, A. E.; Dym, O.; Castrucci, A. M.; Hintz, M. F.; Riehm, J. P.; Rao, K. R. *J. Med. Chem.* **1987**, *30*, 2126–2130.
- (39) Castrucci, A. M.; Hadley, M. E.; Sawyer, T. K.; Wilkes, B. C.; Al-Obeidi, F.; Staples, D. J.; de Vaux, A. E.; Dym, O.; Hintz, M. F.; Riehm, J. P.; Rao, K. R.; Hruby, V. J. *Gen. Comp. Endocrinol.* **1989**, *73*, 157–163.
- (40) Hruby, V. J.; Cai, M.; Grieco, P.; Han, G.; Kavarana, M.; Trivedi, D. *Ann. N.Y. Acad. Sci.* **2003**, *994*, 12–20.
- (41) Hruby, V. J.; Cai, M.; Cain, J. P.; Mayorov, A. V.; Dedek, M. M.; Trivedi, D. *Curr. Top. Med. Chem.* **2007**, *7*, 1107–1119.
- (42) Rajeswaran, W. G.; Hocart, S. J.; Murphy, W. A.; Taylor, J. E.; Coy, D. H. *J. Med. Chem.* **2001**, *44*, 1416–1421.
- (43) Laufer, R.; Gilon, C.; Chorev, M.; Selinger, Z. *J. Biol. Chem.* **1986**, *261*, 10257–10263.
- (44) Laufer, R.; Wormser, U.; Friedman, Z. Y.; Gilon, C.; Chorev, M.; Selinger, Z. *Proc. Natl. Acad. Sci. U.S.A.* **1985**, *82*, 7444–7448.
- (45) Kawasaki, A. M.; Knapp, R.; Wire, W.; Kramer, T.; Yamamura, H. I.; Burks, T. F.; Hruby, V. J. *Peptides: Chemistry, Structure and Biology, Proceedings of the Eleventh American Peptide Symposium 1990*, 337–338.
- (46) Hruby, V. J.; Fang, S. A.; Knapp, R.; Kazimierski, W.; Lui, G. K.; Yamamura, H. I. *Int. J. Pept. Protein Res.* **1990**, *35*, 566–573.
- (47) Knapp, R. J.; Vaughn, L. K.; Fang, S. N.; Bogert, C. L.; Yamamura, M. S.; Hruby, V. J.; Yamamura, H. I. *J. Pharmacol. Exp. Ther.* **1990**, *255*, 1278–1286.
- (48) Chatterjee, J.; Ovadia, O.; Zahn, G.; Marinelli, L.; Hoffman, A.; Gilon, C.; Kessler, H. *J. Med. Chem.* **2007**, *50*, 5878–5881.
- (49) Cody, W. L.; He, J. X.; Reily, M. D.; Haleen, S. J.; Walker, D. M.; Reyner, E. L.; Stewart, B. H.; Doherty, A. M. *J. Med. Chem.* **1997**, *40*, 2228–2240.
- (50) Haviv, F.; Fitzpatrick, T. D.; Swenson, R. E.; Nichols, C. J.; Mort, N. A.; Bush, E. N.; Diaz, G.; Bammert, G.; Nguyen, A.; Rhutasel, N. S.; Nellans, H. N.; Hoffman, D. J.; Johnson, E. S.; Greer, J. J. *Med. Chem.* **1993**, *36*, 363–369.
- (51) Fairlie, D. P.; Abbenante, G.; March, D. R. *Curr. Med. Chem.* **1995**, *2*, 654–686.
- (52) Tonelli, A. E. *Biopolymers* **1976**, *15*, 1615–1622.
- (53) Manavalan, P.; Momany, F. A. *Biopolymers* **1980**, *19*, 1943–1973.
- (54) Ron, D.; Gilon, C.; Hanani, M.; Vromen, A.; Selinger, Z.; Chorev, M. *J. Med. Chem.* **1992**, *35*, 2806–2811.
- (55) Dechantsreiter, M. A.; Planker, E.; Mathä, B.; Lohof, E.; Hölzemann, G.; Jonczyk, A.; Goodman, S. L.; Kessler, H. *J. Med. Chem.* **1999**, *42*, 3033–3040.
- (56) Ali, F. E.; Bennett, D. B.; Calvo, R. R.; Elliott, J. D.; Hwang, S. M.; Ku, T. W.; Lago, M. A.; Nichols, A. J.; Romoff, T. T.; Shah, D. H.; Vasko, J. A.; Wong, A. S.; Yellin, T. O.; Yuan, C.-K.; Samanen, J. M. *J. Med. Chem.* **1994**, *37*, 769–780.
- (57) Mazur, R. H.; James, P. A.; Tyner, D. A.; Hallinan, E. A.; Sanner, J. H.; Schulze, R. *J. Med. Chem.* **1980**, *23*, 758–763.

formational rigidity.^{48,51,58} It may also turn an agonist into an antagonist.⁵⁷

Application of the *N*-alkyl scan concept⁵⁹ to the highly active and selective cyclic pentapeptide cyclo(-RGDFV-)⁶⁰ has led to one of the most active (0.5 nM) and selective inhibitors for the $\alpha_v\beta_3$ integrin,^{55,61} the analog cyclo(-Arg-Gly-Asp-D-Phe-(Me)-Val-), Cilengitide,^{55,61} which is now in clinical phase III for treatment of glioblastoma. *N*-Alkylation is also present in naturally occurring peptides from plants, marine sources and various microorganisms. Several of these compounds exhibit biological activity like antibiotic,^{62–64} antitumor^{65–67} and immunosuppressor activity.⁶⁸

Peptide Design. Ac-Nle⁴-c[Asp⁵, D-Phe⁷, Lys¹⁰]- α -MSH(4–10)-NH₂ (MT-II) was chosen as a template for the design of a combinatorial library to search for more selective melanotropin peptides. Some *N*-methyl amino acids are commercially available, but most are expensive. However, several methods for synthesizing *N*-methylated amino acids in solution and on solid supports have been developed.⁶⁹ We decided to do the *N*-methylations on a solid support, which gives flexibility in library design and facilitated coupling, because no coupling of *N*-methylated amino acids to an *N*-methylated peptide is necessary.⁶ We used the procedure originally described by Miller and Scanlan⁷⁰ which has been optimized by Biron et al. and which is compatible with all commonly used amino acids.⁷¹

A major advantage of the *o*-NBS protecting group coupled to the free amine prior to *N*-methylation is that deprotection with mercaptoethanol is selective for *N*-methylated derivatives and does not occur when the protected amine is not alkylated.⁷¹ Hence, it provides an inherent purification step during synthesis.

Couplings on *N*^α-methylamino acids are known to be more challenging than normal couplings.⁷² Hence, these couplings were performed with HATU and HOAt instead of TBTU and HOBt using DIEA as base in NMP yielding in complete couplings after 3 h. Nevertheless, some peptides (**3**, **13**, **25**) could not be purified as sharp peaks by HPLC and were

observed as broad peaks or mixtures of two peaks with identical mass, even after repeated synthesis. When the peaks were separated and reinjected, similar chromatograms were observed. This indicated the presence of conformational isomers rather than diastereomers. To study the influence of *N*-methylation on the conformation of the pharmacophore of MT-II, a library of MT-II analogues with single and multiple *N*-methylation in the core sequence of MT-II has been designed and synthesized (Figure 1 and Table 1).

Results and Discussion

Biological Data. Competitive binding assays with [¹²⁵I]-[Nle⁴,D-Phe⁷]- α -MSH (NDP- α -MSH), and adenylate cyclase assays were performed on HEK293 cells stably expressing the hMC1R, hMC3R, hMC4R, and hMC5R (Table 1 and Table 2, respectively).

In the first group of peptides with the single *N*-methylation screen (peptides **2–6**), it is revealed that *N*-Me-D-Phe caused a total loss of binding as well as adenylate cyclase activities (Tables 1 and 2) at the hMC1R, hMC3R, hMC4R and hMC5R for peptide **5**. For the rest of the core sequence single *N*-methylation does not cause this drastic loss of binding activities (Table 1). The cAMP assay data (Table 2) show that the *N*-methylated peptides **2**, **3** and **6** still retain full agonist or partial agonist activity toward all subtypes of melanocortin receptors. This phenomenon parallels earlier studies that have shown that D-Phe is the most critical amino acid for the binding and cAMP activities to hMCRs.^{43,73,75} The *N*-Me-D-Phe⁷ substitution apparently led to a conformation which prevents interaction of the aromatic ring with the third and the sixth transmembrane binding domains aromatic groups.⁷⁶ The *N*-Me-His⁶ analog reveals increased binding selectivity for the hMC1R and hMC3R. This result parallels our earlier observation that constraining the His residue can lead to potent antagonists especially for the hMC3R.⁷⁷

The second group of peptides are dimethylated derivatives in the core sequence of MT-II (peptides **7–16**). In this group, some exciting results are observed. It is first demonstrated that any site of *N*-methylation combined with *N*-Me-D-Phe⁷ will lose the binding as well as cAMP activities at all hMCRs (peptides **9**, **12**, **14**, **16**) confirming the results from monomethylation. *N*-Methylation combined with *N*-Me-Lys reduces binding at the hMC4R and hMC5R (peptide **7**, **8**, **10**). The cAMP functional assays show that except **7** at the hMC5R these peptides retain partial agonist activities. *N*-Methylation combined with *N*-Me-Trp increases the selective agonist activity at the hMC1R (peptides **11**, **13**), and selective antagonist activity at hMC3R (peptide **13**) and lead to large decreases in binding and functional activity at the hMC4R and hMC5R resulting in increased selectivity of peptide **12** for the hMC3R. The combination of *N*-Me-His and *N*-Me-Arg (peptide **15**) reduces the binding at

(58) Vitoux, B.; Aubry, A.; Cung, M. T.; Marraud, M. *Int. J. Pept. Protein Res.* **1986**, *27*, 617–632.

(59) Sugano, H.; Higaki, K.; Miyoshi, M. *Bull. Chem. Soc. Jpn.* **1973**, *46*, 226–230.

(60) Aumailley, M.; Gurrath, M.; Müller, G.; Calvete, J.; Timpl, R.; Kessler, H. *FEBS Lett.* **1991**, *291*, 50–54.

(61) Dechantsreiter, M. A.; Mathä, B.; Jonczyk, A.; Goodman, S. L.; Kessler, H. *Peptides 1996*; Mayflower Scientific: Kingswinford, 1996; p 329.

(62) Shemyakin, M. M.; Ovchinnikov, Y. A.; Ivanov, V. T.; Kiryushkin, A. A. *Tetrahedron* **1963**, *19*, 581–591.

(63) Bevan, K.; Davies, J. S.; Hall, M. J.; Hassall, C. H.; Morton, R. B.; Phillips, D. A.; Ogihara, Y.; Thomas, W. A. *Experientia* **1970**, *26*, 122–123.

(64) Corbaz, R.; Ettliger, L.; Gaumann, E.; Keller-Schierlein, W.; Kradolfer, F.; Neipp, L.; Prelog, V. *Helv. Chim. Acta* **1957**, *23*, 199.

(65) Jolad, S. D.; Hoffmann, J. J.; Torrance, S. J.; Wiedhopf, R. M.; Cole, J. R.; Arora, S. K.; Bates, R. B.; Gargiulo, R. L.; Kriek, G. R. *J. Am. Chem. Soc.* **1977**, *99*, 8040–8044.

(66) Pettit, G. R.; Kamano, Y.; Dufresne, C.; Cerny, R. L.; Herald, C. L.; Schmidt, J. M. *J. Org. Chem.* **1989**, *54*, 6005.

(67) Pettit, G. R.; Kamano, Y.; Herald, C. L.; Tuinman, A. A.; Boettner, F. E.; Kizu, H.; Schmidt, J. M.; Baczynskyj, L.; Tomer, K. B.; Bontems, R. J. *J. Am. Chem. Soc.* **1987**, *109*, 6883–6885.

(68) Ruegger, A.; Kuhn, M.; Lichti, H.; Loosli, H.-R.; Huguenin, R.; Quiquerez, C.; von Wartburg, A. *Helv. Chim. Acta* **1976**, *59*, 1075.

(69) Biron, E.; Kessler, H. *J. Org. Chem.* **2005**, *70*, 5183–5189.

(70) Miller, S. C.; Scanlan, T. S. *J. Am. Chem. Soc.* **1997**, *119*, 2301–2302.

(71) Biron, E.; Chatterjee, J.; Kessler, H. *J. Pept. Sci.* **2006**, *12*, 213–219.

(72) Teixido, M.; Albericio, F.; Giralt, E. *J. Pept. Res.* **2005**, *65*, 153–166.

(73) Haskell-Luevano, C.; Miwa, H.; Dickinson, C.; Hruby, V. J.; Yamada, T.; Gantz, I. *Biochem. Biophys. Res. Commun.* **1994**, *204*, 1137–1142.

(74) Haskell-Luevano, C.; Sawyer, T. K.; Hendrata, S.; North, C.; Panahinia, L.; Stum, M.; Staples, D. J.; Castrucci, A. M.; Hadley, M. F.; Hruby, V. J. *Peptides* **1996**, *17*, 995–1002.

(75) Sawyer, T. K.; Sanfilippo, P. J.; Hruby, V. J.; Engel, E. H.; Heward, C. B.; Burnett, J. B.; Hadley, M. E. *Proc. Natl. Acad. Sci. U.S.A.* **1980**, *77*, 5754–5758.

(76) Chen, M.; Cai, M.; Aprahamian, C. J.; Georgeson, K. E.; Hruby, V.; Harmon, C. M.; Yang, Y. *J. Biol. Chem.* **2007**, *282*, 21712–21719.

(77) Grieco, P.; Cai, M.; Han, G.; Trivedi, D.; Campiglia, P.; Novellino, E.; Hruby, V. J. *Peptides* **2007**, *28*, 1191–1196.

Table 1. Binding Assay of *N*-Methylated MT-II Analogues at hMCRs^a

Sequence	hMCR1R			hMCR3R			hMCR4R			hMCR5R		
	IC ₅₀ (nM)	Percent Binding Efficiency	Percent Binding Efficiency	IC ₅₀ (nM)	Percent Binding Efficiency	Percent Binding Efficiency	IC ₅₀ (nM)	Percent Binding Efficiency	Percent Binding Efficiency	IC ₅₀ (nM)	Percent Binding Efficiency	Percent Binding Efficiency
1 Ac-Nle-c[D-H-f-R-W-K]	3.5 ± 0.23	100.0 ± 0.00	100.0 ± 0.00	6.8 ± 0.87	100.0 ± 0.00	100.0 ± 0.00	4.2 ± 1.06	100.0 ± 0.00	100.0 ± 0.00	12.1 ± 2.28	100.0 ± 0.00	100.0 ± 0.00
2 Ac-Nle-c[D-H-f-R-W-Kα]	6.70 ± 100	100 ± 20	98 ± 0.58	23 ± 4.5	98 ± 0.58	88 ± 32	88 ± 32	99 ± 1.5	77 ± 29	77 ± 29	99 ± 1.5	97 ± 0.43
3 Ac-Nle-c[D-H-f-R-W-K]	88 ± 11	100 ± 10	100 ± 10	27 ± 3	100 ± 10	1700 ± 16	1700 ± 16	100	780	780	100	100 ± 10
4 Ac-Nle-c[D-H-f-R-W-K]	90 ± 11	100 ± 20	100 ± 10	14 ± 1	100 ± 10	2000	2000	100	450	450	100	89 ± 6
5 Ac-Nle-c[D-H-f-R-W-K]	NB	NB	NB	NB	NB	NB	NB	NB	NB	NB	NB	NB
6 Ac-Nle-c[D-H-f-R-W-K]	100 ± 20	97	100 ± 11	37 ± 1	100 ± 11	1300	1300	1101 ± 100	3400	3400	1101 ± 100	85 ± 6
7 Ac-Nle-c[D-H-f-R-W-Kα]	4.3 ± 1.6	98 ± 0.12	65 ± 4.6	65 ± 4.6	98 ± 1.7	370 ± 120	370 ± 120	10 ± 0.15	2200 ± 330	2200 ± 330	10 ± 0.15	78 ± 2
8 Ac-Nle-c[D-H-f-R-W-Kα]	12 ± 4	100 ± 20	28 ± 1	28 ± 1	100 ± 1	720 ± 80	720 ± 80	100 ± 9	840 ± 100	840 ± 100	100 ± 9	89 ± 10
9 Ac-Nle-c[D-H-f-R-W-Kα]	NB	NB	NB	NB	NB	NB	NB	NB	NB	NB	NB	NB
10 Ac-Nle-c[D-H-f-R-W-Kα]	270 ± 30	100	200 ± 64	200 ± 64	72 ± 16	1300 ± 150	1300 ± 150	91 ± 9	580 ± 380	580 ± 380	91 ± 9	63 ± 14
11 Ac-Nle-c[D-H-f-R-W-K]	6.7 ± 0.38	89 ± 0.97	13 ± 1	13 ± 1	69 ± 5	440 ± 50	440 ± 50	54 ± 9	1600 ± 110	1600 ± 110	54 ± 9	87 ± 55
12 Ac-Nle-c[D-H-f-R-W-K]	NB	NB	890 ± 180	890 ± 180	84 ± 3.2	NB	NB	NB	NB	NB	NB	NB
13 Ac-Nle-c[D-H-f-R-W-K]	56 ± 26	98 ± 0.78	81 ± 24	81 ± 24	98 ± 1.54	NB	NB	NB	130 ± 11	130 ± 11	NB	80 ± 77
14 Ac-Nle-c[D-H-f-R-W-K]	6700 ± 3400	73 ± 3.5	1400 ± 100	1400 ± 100	77 ± 8	NB	NB	NB	840 ± 33	840 ± 33	NB	81 ± 22
15 Ac-Nle-c[D-H-f-R-W-K]	35 ± NA	100 ± NA	120 ± 100	120 ± 100	97 ± 9	1700 ± 200	1700 ± 200	88 ± 9	1800 ± 200	1800 ± 200	88 ± 9	92 ± 10
16 Ac-Nle-c[D-H-f-R-W-K]	NB	NB	NB	NB	NB	NB	NB	NB	NB	NB	NB	NB
17 Ac-Nle-c[D-H-f-R-W-Kα]	8.2 ± 4.6	100 ± 1.9	120 ± 22	120 ± 22	94 ± 1.9	400 ± 190	400 ± 190	890 ± 66	200 ± 28	200 ± 28	890 ± 66	95 ± 32
18 Ac-Nle-c[D-H-f-R-W-Kα]	NB	NB	NB	NB	NB	NB	NB	NB	NB	NB	NB	NB
19 Ac-Nle-c[D-H-f-R-W-Kα]	190 ± 92	92 ± 6.3	1900 ± 200	1900 ± 200	83 ± 3	NB	NB	43 ± 4	580 ± 81	580 ± 81	43 ± 4	83 ± 1.4
20 Ac-Nle-c[D-H-f-R-W-Kα]	NB	NB	NB	NB	NB	NB	NB	NB	NB	NB	NB	NB
21 Ac-Nle-c[D-H-f-R-W-Kα]	31 ± 8.1	88 ± 67	320 ± 20	320 ± 20	95 ± 10	6000 ± 100	6000 ± 100	65 ± 6	215 ± 84	215 ± 84	65 ± 6	83 ± 11
22 Ac-Nle-c[D-H-f-R-W-Kα]	NB	NB	NB	NB	NB	NB	NB	NB	NB	NB	NB	NB
23 Ac-Nle-c[D-H-f-R-W-K]	NB	NB	NB	NB	NB	NB	NB	NB	NB	NB	NB	NB
24 Ac-Nle-c[D-H-f-R-W-K]	57 ± 12	95 ± 1.1	NB	NB	95 ± 1.1	NB	NB	NB	NB	NB	NB	NB
25 Ac-Nle-c[D-H-f-R-W-K]	NB	NB	NB	NB	NB	NB	NB	NB	NB	NB	NB	NB
26 Ac-Nle-c[D-H-f-R-W-K]	NB	NB	NB	NB	NB	NB	NB	NB	620 ± 60	620 ± 60	NB	95 ± 10
27 Ac-Nle-c[D-H-f-R-W-Kα]	2500 ± 110	55 ± 10	NB	NB	NB	NB	NB	NB	NB	NB	NB	NB
28 Ac-Nle-c[D-H-f-R-W-Kα]	14 ± 4.0	95 ± 1	2200 ± 480	2200 ± 480	95 ± 4.2	NB	NB	NB	NB	NB	NB	NB
29 Ac-Nle-c[D-H-f-R-W-Kα]	NB	NB	NB	NB	NB	NB	NB	NB	690 ± 70	690 ± 70	NB	92 ± 10
30 Ac-Nle-c[D-H-f-R-W-Kα]	NB	NB	NB	NB	NB	NB	NB	NB	720 ± 80	720 ± 80	NB	100 ± 10
31 Ac-Nle-c[D-H-f-R-W-K]	NB	NB	NB	NB	NB	NB	NB	NB	NB	NB	NB	NB
32 Ac-Nle-c[D-H-f-R-W-Kα]	NB	NB	NB	NB	NB	NB	NB	NB	160 ± 20	160 ± 20	NB	89 ± 8
33 Ac-Nle-c[D-H-f-R-W-Ks]	1.7 ± 0.21	97 ± 1.2	6.8 ± 0.25	6.8 ± 0.25	98 ± 1.2	3200 ± 580	3200 ± 580	33 ± 1.3	9.3 ± 0.01	9.3 ± 0.01	33 ± 1.3	96.0 ± 4.2

^a Gray highlighted amino acids are *N*-methylated. IC₅₀ = concentration of peptide at 50% specific binding (*N* = 4). NB = 0% of [¹²⁵I]-NDP-α-MSH displacement observed at 10 μM. Percent Binding Efficiency = maximal % of [¹²⁵I]-NDP-α-MSH displacement observed at 10 μM.

Table 2. cAMP Assay of N-Methylated MT-II Analogues at hMCRs^a

Sequence	hMC1R		hMC3R		hMC4R		hMC5R	
	EC ₅₀ (nM)	Percent Activity	EC ₅₀ (nM)	Percent Activity	EC ₅₀ (nM)	Percent Activity	EC ₅₀ (nM)	Percent Activity
1 Ac -Nle -c[D - H - f - R - W - K]	2.0±0.38	100	5.6±1.9	100	7.3±1.5	100	5.6±1.1	100
2 Ac -Nle -c[D - H - f - R - W - Kα]	1.1±0.30	100±2.7	62±6.5	52±6.2	62±2.2	78±8.	3.7±0.77	82±8.6
3 Ac -Nle -c[D - H - f - R - W - K]	1.8±0.40	77±13	2.1±0.2	100±1	19±15	86±33	5.6±2.5	66±12
4 Ac -Nle -c[D - H - f - R - W - K]	1.7±0.03	60±2	3.4±2.1	97±11	3.3±0.3	73±10	6.0±2.2	77±19
5 Ac -Nle -c[D - H - f - R - W - K]	NA	NA	NA	NA	NA	NA	NA	NA
6 Ac -Nle -c[D - H - f - R - W - K]	5.3±1.3	58±12	9400	260	79±7	55±5	22±16	73±14
7 Ac -Nle -c[D - H - f - R - W - Kα]	7.6±6.0	79±36	47±36	25±4.	100±10	80±8	NA	NA
8 Ac -Nle -c[D - H - f - R - W - Kα]	9.5±7.7	100±1.3	19	60	27±3	53±5	12±1	53±2
9 Ac -Nle -c[D - H - f - R - W - Kα]	NA	NA	NA	NA	NA	NA	NA	NA
10 Ac -Nle -c[D - H - f - R - W - Kα]	13±9.8	70±28	19	90	470±36	83±13	1000±100	67±3
11 Ac -Nle -c[D - H - f - R - W - K]	2.7±0.04	100±5	61±35.	58±8.7	440±220	86±11	420±220	65±1
12 Ac -Nle -c[D - H - f - R - W - K]	NA	NA	800±760	84±5.5	NA	NA	NA	NA
13 Ac -Nle -c[D - H - f - R - W - K]	18±16	110±7.0	7.0	20±3	NA	NA	NA	NA
14 Ac -Nle -c[D - H - f - R - W - K]	110±20	77±1	570	85±10	9200±6000	130±33	1400±69	58±14
15 Ac -Nle -c[D - H - f - R - W - K]	13±10	97±10	4.6	75±8	370±50	43±5	480±50	71
16 Ac -Nle -c[D - H - f - R - W - K]	NA	NA	NA	NA	NA	NA	NA	NA
17 Ac -Nle -c[D - H - f - R - W - Kα]	1.8±1.3	78±24	120±21	19±6.4	NA	NA	400±360	78±2.1
18 Ac -Nle -c[D - H - f - R - W - Kα]	NA	NA	NA	NA	NA	NA	NA	NA
19 Ac -Nle -c[D - H - f - R - W - Kα]	18±3.5	100±0.25	NA	NA	1600±500	62±24	NA	NA
20 Ac -Nle -c[D - H - f - R - W - Kα]	NA	NA	NA	NA	NA	NA	NA	NA
21 Ac -Nle -c[D - H - f - R - W - Kα]	2.3±1.2	88±11	NA	NA	290±30	65±1	220±180	47±5
22 Ac -Nle -c[D - H - f - R - W - Kα]	NA	NA	NA	NA	NA	NA	NA	NA
23 Ac -Nle -c[D - H - f - R - W - K]	NA	NA	NA	NA	NA	NA	NA	NA
24 Ac -Nle -c[D - H - f - R - W - K]	40±18	100±8.	NA	NA	NA	NA	NA	NA
25 Ac -Nle -c[D - H - f - R - W - K]	NA	NA	NA	NA	NA	NA	NA	NA
26 Ac -Nle -c[D - H - f - R - W - K]	NA	NA	NA	NA	NA	NA	520±60	6±1
27 Ac -Nle -c[D - H - f - R - W - Kα]	750±280	87±25	NA	NA	NA	NA	NA	NA
28 Ac -Nle -c[D - H - f - R - W - Kα]	13±10	98±66	NA	NA	NA	NA	NA	NA
29 Ac -Nle -c[D - H - f - R - W - Kα]	NA	NA	NA	NA	NA	NA	NA	NA
30 Ac -Nle -c[D - H - f - R - W - Kα]	670±150	42±13	NA	NA	NA	NA	NA	NA
31 Ac -Nle -c[D - H - f - R - W - K]	NA	NA	NA	NA	NA	NA	NA	NA
32 Ac -Nle -c[D - H - f - R - W - Kα]	NA	NA	NA	NA	NA	NA	NA	NA
33 Ac -Nle -c[D - H - f - R - W - Ks]	1.8±1.2	99±4.6	9.1±4.8	68±43	NA	NA	NA	NA

^a Gray highlighted amino acids are N-methylated. EC₅₀ = Effective concentration of peptide that was able to generate 50% maximal intracellular cAMP accumulation (N = 4). Percent Activity = % of cAMP produced at 10 μM ligand concentration, in relation to MT-II. NA = 0% cAMP accumulation observed at 10 μM. The peptides were tested at a range of concentration from 10⁻¹⁰ to 10⁻⁵ M.

the hMC4R and the hMC5R, therefore increase the agonist selectivity for the hMC1R and hMC3R.

More interesting results are found in the third group of peptides (peptides 17–26), tri-*N*-methylated derivatives in the core sequence of MT-II caused a loss in binding affinities (peptides 18, 20, 22, 23, 25, 26), especially, with any of the combinations with *N*-Me-D-Phe. In this group, as long as D-Phe is not *N*-methylated, most ligands will retain binding activity at hMCRs (peptides 17, 19, 21, 24), but they all have reduced cAMP activity (Table 2) except at the hMC1R (partial agonists). Tri-*N*-methylations generally increase the agonist selectivity for the hMC1R (peptides 17, 19, 21, 24). It can be seen from Table 1 that 24 has totally lost activity for all receptors but the hMC1R, which still exhibits good binding affinity and >1000 fold selectivity vs the hMC3, hMC4 and hMC5 receptors. The compound has agonist activity as well (Table 2).

Selectivity, but also loss of activity, are further shown for the five tetra-*N*-methylated MT-II derivatives (peptides 27–31). Tetra-*N*-methylation caused a loss in binding affinities and cAMP activities at all subtypes of hMCRs except for peptide 28, which has potent binding affinity (14 nM) at the hMC1R and has full agonist activity. Thus, a highly potent and selective agonist of hMC1R has been obtained. Peptides 29, 30 and especially 32 are weak, but selective antagonists for the hMC5R.

In addition to 31 *N*^ε-methylated analogs, one ε-*N*-methylated lysine analogue (peptide 33) was investigated. It is interesting to note that in the case of peptide 33, there was a loss in binding to the hMC4R, while selective antagonist activity was seen for the hMC5R in the nanomolar range (peptide 33 is still a full agonist at the hMC1R and the hMC3R). Thus far there are a few cases of selective peptide antagonists at the hMC5R.

It has been demonstrated that the MC1R, which is activated selectively by the 4-fold *N*-methylated peptide 28 is involved in pain, in immune response, and in melanoma cancer.⁷⁸ Thus, highly selective MC1R ligands have potential for treatment of pigmentary disorders,^{18–20,79,80} treatment of pain,⁷⁸ cancer therapy,^{81,82} and inflammatory disorders of the skin. The hMC1R is just one subtype of hMCRs in the melanocortin system. It is mainly distributed in the peripheral system in mammals, and the other subtypes of hMCRs are distributed in both of the peripheral and the central nervous system.¹⁸ Designing highly constrained, lipophilic hMC1R selective *N*-methylated MT-II derivatives will have widest application for specific targeting of disease.

NMR Conformational Studies. The conformation of the highly potent and selective compound 28 (Figure 2) was investigated by NMR spectroscopy, restrained distance geometry calculations (DG), restrained 150 ps MD simulation in explicit water (rMD) and by unrestrained 30 ns MD simulation in explicit water (MD). Based on NMR assignments (Table 3) and other NMR data (ROEs, homo- and heteronuclear scalar

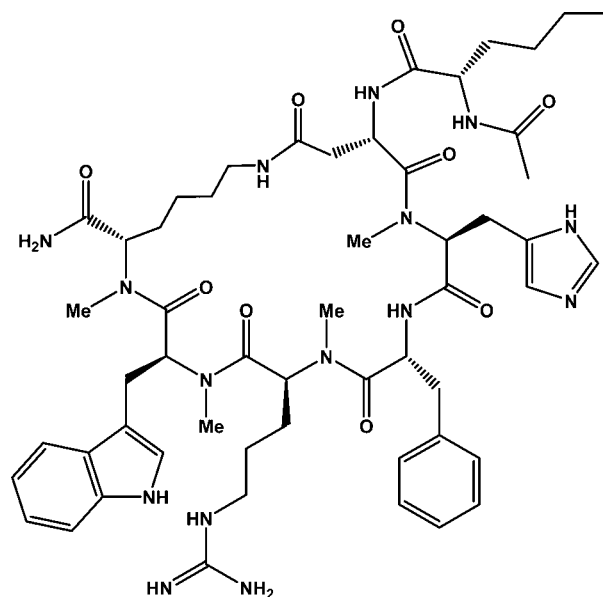


Figure 2. Molecular structure of compound 28.

coupling constants, H^N temperature gradients) and on restrained and unrestrained molecular dynamics a distinct and preferred structure could be derived for the peptide backbone. The amide bridged side chains of the residues Asp⁵ and *N*-Me-Lys¹⁰ that are also part of the cyclic core were found to be flexible. The resulting good agreement between measured and calculated distances clearly indicates a preferred backbone conformation of the structure obtained from the restrained MD simulation (Table 4).⁸³ In a very extended (30 ns) unrestrained MD simulation in explicit water this structure proved to be stable except for slight changes of four backbone dihedral angles in the range of 20–40° (Table 5). Indicators for a reliable structure can be seen in the predominantly parallel orientation of CO(*i*) to C^αH^α(*i* + 1) bond vectors⁸⁴ and in an overall high dispersion of backbone chemical shifts ($H^α$: 4.231 to 6.021 ppm (Figure 3), H^{Me} : 1.559 to 3.115 ppm). In our hands a comparative attempt to discuss the spectral data of non-*N*-methylated MT-II by one single preferred conformation failed. There was considerable backbone dynamics as indicated by a high heterogeneity of the best 30 out of 50 MT-II conformers obtained from DG calculations (rmsd of the backbone carbon and nitrogen atoms of 1.26 Å). Moreover, a low dispersion of chemical shifts ($H^α$: 4.198 to 4.644 ppm (Figure 3), H^N : 7.871 to 8.541 ppm), a lack of strong differentiation of all seven backbone H^N temperature gradients (−8.61 to −5.24 ppb/K) and of amide proton exchange rates as estimated by ROESY exchange peaks, as well as a smaller preference of distinct side chain conformations was observed. Altogether, these indicators suggest a more flexible peptide backbone of MT-II as compared to peptide 28.

Structure of the Peptide Backbone of 28. The conformation of compound 28 is shown in Figure 4. The ROE pattern demonstrates that all peptide bonds are *trans* configured. As most of the amide bonds are *N*-methylated, turn-structures are not only defined by intramolecular hydrogen bonds.⁸⁵ We think

(78) Mogil, J. S.; Wilson, S. G.; Chesler, E. J.; Rankin, A. L.; Nemmani, K. V. S.; Lariviere, W. R.; Groce, M. K.; Wallace, M. R.; Kaplan, L.; Staud, R.; Ness, T. J.; Glover, T. L.; Stankova, M.; Mayorov, A.; Hruby, V. J.; Grisel, J. E.; Fillingim, R. B. *Proc. Natl. Acad. Sci. U.S.A.* **2003**, *100*, 4867–4872.

(79) Dorr, R. T.; Dvorakova, K.; Brooks, C.; Lines, R.; Levine, N.; Schram, K.; Miketova, P.; Hruby, V. J.; Alberts, D. S. *Photochem. Photobiol.* **2000**, *72*, 526–532.

(80) Hadley, M. E.; Hruby, V. J.; Sharma, S. D.; Dorr, R. T.; Levine, N. *Ann. N.Y. Acad. Sci.* **1993**, *680*, 424–439.

(81) Sharma, S. D.; Jiang, J.; Hadley, M. E.; Bentley, D. L.; Hruby, V. J. *Proc. Natl. Acad. Sci. U.S.A.* **1996**, *93*, 13715–13720.

(82) Jiang, J.; Sharma, S. D.; Fink, J. L.; Hadley, M. E.; Hruby, V. J. *Exp. Dermatol.* **1996**, *5*, 325–333.

(83) Kessler, H.; Griesinger, C.; Lautz, J.; Müller, A.; van Gunsteren, W. F.; Berendsen, H. J. C. *J. Am. Chem. Soc.* **1988**, *110*, 3393–3396.

(84) Heller, M.; Sukopp, M.; Tsomaia, N.; John, M.; Mierke, D. F.; Reif, B.; Kessler, H. *J. Am. Chem. Soc.* **2006**, *128*, 13806–13814.

(85) Matthews, B. W. *Macromolecules* **1972**, *5*, 818–819.

Table 3. Resonance Assignment of Peptide **28** (Sodium Acetate-d4 Buffer (50 mM), pH 4.5, 298 K)^a

	H ^N (H ^{NMe})	H ^α	H ^β	H ^γ	H ^δ	H ^ε	H ^ζ	H ^η	others
Nle ⁴	8.166	4.231	1.653 1.701	1.281	1.320	0.893	—	—	H ^{Acetyl} : 2.062
Asp ⁵	8.328	5.183	proR: 2.271 proS: 2.521	—	—	—	—	—	—
N-Me-His ⁶	(3.115)	5.392	proR: 3.272 proS: 3.063	—	2: 7.084	1: 8.563	—	—	—
D-Phe ⁷	7.657	4.668	proR: 2.901 proS: 2.661	—	7.152	7.327	7.320	—	—
N-Me-Arg ⁸	(1.559)	5.164	proR: 1.245 proS: 1.518	1.168 1.255	3.084	7.144	—	—	—
N-Me-Trp ⁹	(2.695)	6.021	proR: 3.287 proS: 3.216	—	1: 7.249	1: 10.180 3: 7.639	2: 7.535 3: 7.150	2: 7.321	—
N-Me-Lys ¹⁰	(2.774)	5.238	1.914 1.914	1.146 1.291	1.470 1.594	3.046 3.530	8.174	—	H ^{Amide} : 7.145 7.575

^a Chemical shifts are referenced on sodium 3-(trimethylsilyl)propionate-2,2,3,3-d4 (¹H at 0.000 ppm).

that steric effects and dipole orientation such as the above-mentioned parallel orientation of CO(*i*) to C^αH^α(*i* + 1) bond vectors⁸⁴ contribute most strongly to the conformation of smaller *N*-methylated cyclic peptides.

According to the *N*-Me-His⁶ backbone dihedral angles ($\Phi = -98^\circ$, $\Psi = 78^\circ$) the structure obtained from restrained MD simulation possesses an inverted γ -turn⁸⁵ centered at *N*-Me-His⁶. A distance of 3.4 Å between the Asp⁵ carbonyl oxygen and the D-Phe⁷ amide nitrogen, a hydrogen bond angle of 141° and a moderately negative temperature gradient of D-Phe⁷ H^N (−5.92 ppb/K in the aqueous buffer, −5.55 ppb/K in DMSO) indicate that the hydrogen bond within this inverted γ -turn is rather weak and protection form the solvent is incomplete. According to the minimal requirement for β -turns,⁸⁶ which consists in a distance of less than 7 Å between C^α_{*i*} and C^α_{*i*+3}, the inverted γ -turn is located within a β -turn ranging from Asp⁵ to *N*-Me-Arg⁸ (C^α–C^α distance: 6.4 Å). A distance of 7.6 Å between the α -carbon atoms of *N*-Me-His⁶ and *N*-Me-Trp⁹ almost fulfills the criterion for a second overlapping β -turn, which is close to type II' β -turn geometry, as D-Phe⁷ Φ , D-Phe⁷ Ψ , *N*-Me-Arg⁸ Φ , and *N*-Me-Arg⁸ Ψ possess dihedral angles of 96°, −126°, −135° and 80°, respectively. The overlapping turns result in a virtually complete helical twist (α -turn) that extends from residues Asp⁵ to *N*-Me-Trp⁹. Hydrophobic clustering of the *N*-Me-Trp⁹ *N*-methyl group with the Asp⁵ H^β, *N*-Me-Arg⁸ H^α, *N*-Me-Lys¹⁰ H^γ atoms and the *N*-Me-His⁶ *N*-methyl group (indicated by the presence of ROESY cross peaks between the *N*-Me-Trp⁹ methyl protons and the Asp⁵ H^β, *N*-Me-Arg⁸ H^α, *N*-Me-Lys¹⁰ H^γ, *N*-Me-His⁶ *N*-methyl protons) seems to stabilize this helical twist. Within the unrestrained 30 ns MD simulation starting from the structure of the restrained MD, slight changes occurred in a few backbone dihedral angles as compared to the average structure from the restrained MD simulation. Asp⁵ Ψ , *N*-Me-His⁶ Ψ , D-Phe⁷ Φ and *N*-Me-Trp⁹ Ψ were most affected and changed from 144° to 113°, 78° to 117°, 96° to 75° and 63° to 96°, respectively (Table 5). The rmsd between the atoms of the peptide backbone from Asp⁵ to *N*-Me-Lys¹⁰ of structures obtained from the unrestrained and restrained MD simulation is 1.0 Å. According to the *N*-Me-His⁶ backbone dihedral angles ($\Phi = -102^\circ$, $\Psi = 117^\circ$) the inverted γ -turn is less pronounced in the structure obtained from unrestrained MD simulation. Upper bounds of some distance restraints within the cyclic core structure (Asp⁵H^β-D-Phe⁷H^N; Asp⁵H^β-*N*-Me-His⁶H^{Me}; D-Phe⁷H^N-*N*-Me-Arg⁸H^α; *N*-Me-Arg⁸H^α-*N*-Me-Lys¹⁰H^{Me}; *N*-Me-Trp⁹H^{Me}-

N-Me-Lys¹⁰H^α) were violated during the unrestrained MD simulation. This can be traced back directly to the aforementioned changes in backbone dihedral angles. As illustrated in more detail in the sections describing the side chain dynamics and structure calculations, we think that the changes in the backbone dihedral angles were caused by artificial strains in the amide linked Asp⁵ and *N*-Me-Lys¹⁰ side chains. These were introduced within the DG calculation as our structure calculation protocol did not take conformational averaging explicitly into account. Accordingly, the conformer obtained from restrained MD seems to be the best structural model for the peptide backbone and we focused the analysis of side chain conformation on this structure.

In consideration of the high binding affinity to hMC1R (IC₅₀ = 14 nM) and the strong restriction that cyclization and 4-fold *N*-methylation pose on conformational changes within the backbone of peptide **28**, we think that its backbone conformation in aqueous solution is very close to the conformation present in the receptor bound state.

The conformation of the peptide backbone also offers an explanation for the strong interference of D-Phe⁷ *N*-methylation with hMCR affinity, as *N*-methylation goes in hand with an increased spatial requirement and increased hydrophobicity in comparison to the replaced amide proton. If D-Phe⁷ is *N*-methylated, these hydrophobic and steric effects would prohibit the formation of the backbone conformation present in peptide **28**, as close proximity between the Asp⁵ carbonyl oxygen and the D-Phe⁷ *N*-methyl group is disfavored. Hence, the *N*-Me-D-Phe⁷ substitution would not simply displace a hydrogen bond donor, but also lead to an altered conformation of the peptide backbone, which would affect the presentation of the pharmacophore and prevent interaction of the aromatic ring with the third and the sixth transmembrane binding domains aromatic groups.⁷⁶

Side Chain Structure and Dynamics. Investigation of side chain conformation about the χ_1 angle requires a careful analysis of homo- and heteronuclear J-couplings as well as the consideration of NOE distances in stereospecifically assigned β protons.⁸⁷ Extended MD simulations of a solution structure in explicit solvent can further clarify which structural flips of side chain dihedral angles are correlated.

The sums of the ³J_{H α -H β} coupling constants of the individual amino acid side chains are in the order of 15 Hz, which excludes

(86) Venkatachalam, C. M. *Biopolymers* **1968**, *6*, 1425–1436.

(87) Kessler, H.; Griesinger, C.; Wagner, K. *J. Am. Chem. Soc.* **1987**, *109*, 6927–6933.

Table 4. Comparison between the Experimentally Derived Distance Restraints (d_{low} , d_{upp}) and Calculated (d_{MD}) Interproton Distances of Compound **28** as obtained from Restrained MD Calculation^a

interproton distance		d_{low} [Å]	d_{upp} [Å]	d_{MD} [Å]	d_{viol} [Å]
Asp ⁵ H ^β _{proR}	Asp ⁵ H ^α	2.32	2.84	2.629	
Asp ⁵ H ^β _{proS}	Asp ⁵ H ^α	2.58	3.15	3.050	
Asp ⁵ H ^α	<i>N</i> -Me-His ⁶ H ^{Me}	2.08	3.19	2.758	
Asp ⁵ H ^β _{proR}	<i>N</i> -Me-His ⁶ H ^α	4.13	5.05	4.635	
Asp ⁵ H ^β _{proR}	<i>N</i> -Me-His ⁶ H ^{Me}	2.52	3.68	3.286	
Asp ⁵ H ^β _{proS}	<i>N</i> -Me-His ⁶ H ^α	4.73	5.78	5.248	
Asp ⁵ H ^α	<i>N</i> -Me-His ⁶ H ^α	4.15	5.07	4.608	
Asp ⁵ H ^β _{proR}	D-Phe ⁷ H ^N	3.15	3.85	3.520	
Asp ⁵ H ^β _{proS}	D-Phe ⁷ H ^N	3.43	4.19	4.100	
Asp ⁵ H ^β _{proR}	<i>N</i> -Me-Trp ⁹ H ^{Me}	2.62	3.78	2.716	
Asp ⁵ H ^α	<i>N</i> -Me-Lys ¹⁰ H ^ξ	3.06	3.74	4.014	+0.27
Asp ⁵ H ^β _{proR}	<i>N</i> -Me-Lys ¹⁰ H ^ξ	2.77	3.38	3.054	
<i>N</i> -Me-His ⁶ H ^{Me}	<i>N</i> -Me-His ⁶ H ^α	3.21	4.43	3.913	
<i>N</i> -Me-His ⁶ H ^α	D-Phe ⁷ H ^N	2.05	2.51	2.390	
<i>N</i> -Me-His ⁶ H ^β	D-Phe ⁷ H ^N	3.71	5.23	4.326	
<i>N</i> -Me-His ⁶ H ^{Me}	D-Phe ⁷ H ^N	3.4	4.64	4.334	
<i>N</i> -Me-His ⁶ H ^α	D-Phe ⁷ H ^α	3.78	4.62	4.500	
<i>N</i> -Me-His ⁶ H ^{Me}	<i>N</i> -Me-Trp ⁹ H ^{Me}	3.24	4.97	3.689	
<i>N</i> -Me-His ⁶ H ^{Me}	<i>N</i> -Me-Trp ⁹ H ^β	3.4	4.64	3.660	
D-Phe ⁷ H ^N	D-Phe ⁷ H ^α	2.53	3.09	3.053	
D-Phe ⁷ H ^β	D-Phe ⁷ H ^N	2.32	3.53	3.187	
D-Phe ⁷ H ^N	<i>N</i> -Me-Arg ⁸ H ^α	3.77	4.61	4.748	+0.14
D-Phe ⁷ H ^α	<i>N</i> -Me-Arg ⁸ H ^{Me}	2.11	3.22	2.679	
D-Phe ⁷ H ^β	<i>N</i> -Me-Arg ⁸ H ^β	3.08	5.16	4.752	
D-Phe ⁷ H ^β	<i>N</i> -Me-Arg ⁸ H ^{Me}	2.65	4.52	4.450	
D-Phe ⁷ H ^α	<i>N</i> -Me-Trp ⁹ H ^α	4.37	5.34	4.472	
<i>N</i> -Me-Arg ⁸ H ^{Me}	<i>N</i> -Me-Arg ⁸ H ^α	3.17	4.39	3.872	
<i>N</i> -Me-Arg ⁸ H ^α	<i>N</i> -Me-Trp ⁹ H ^{Me}	2.08	3.18	2.779	
<i>N</i> -Me-Arg ⁸ H ^β	<i>N</i> -Me-Trp ⁹ H ^α	4.23	5.87	5.526	
<i>N</i> -Me-Arg ⁸ H ^{Me}	<i>N</i> -Me-Trp ⁹ H ^α	3.98	5.29	5.034	
<i>N</i> -Me-Arg ⁸ H ^{Me}	<i>N</i> -Me-Trp ⁹ H ^{Me}	3.34	5.06	4.816	
<i>N</i> -Me-Arg ⁸ H ^α	<i>N</i> -Me-Trp ⁹ H ^α	3.75	4.59	4.579	
<i>N</i> -Me-Arg ⁸ H ^{Me}	<i>N</i> -Me-Trp ⁹ H ^β	3.3	4.53	4.760	+0.23
<i>N</i> -Me-Arg ⁸ H ^{Me}	<i>N</i> -Me-Trp ⁹ H ^α	3.27	4.5	4.184	
<i>N</i> -Me-Arg ⁸ H ^{Me}	<i>N</i> -Me-Trp ⁹ H ^β	3.63	4.9	4.359	
<i>N</i> -Me-Arg ⁸ H ^{Me}	<i>N</i> -Me-Trp ⁹ H ^γ	3.6	4.86	4.123	
<i>N</i> -Me-Arg ⁸ H ^{Me}	<i>N</i> -Me-Trp ⁹ H ^δ	3.45	4.7	3.806	
<i>N</i> -Me-Arg ⁸ H ^{Me}	<i>N</i> -Me-Trp ⁹ H ^ε	2.89	4.08	4.327	+0.25
<i>N</i> -Me-Arg ⁸ H ^α	<i>N</i> -Me-Lys ¹⁰ H ^{Me}	3.32	4.56	4.472	
<i>N</i> -Me-Arg ⁸ H ^β	<i>N</i> -Me-Lys ¹⁰ H ^{Me}	3.26	5.19	5.333	+0.14
<i>N</i> -Me-Trp ⁹ H ^{Me}	<i>N</i> -Me-Trp ⁹ H ^α	3.15	4.37	3.905	
<i>N</i> -Me-Trp ⁹ H ^α	<i>N</i> -Me-Lys ¹⁰ H ^{Me}	2.23	3.35	2.996	
<i>N</i> -Me-Trp ⁹ H ^{Me}	<i>N</i> -Me-Lys ¹⁰ H ^α	3.56	4.83	4.889	+0.06
<i>N</i> -Me-Trp ⁹ H ^{Me}	<i>N</i> -Me-Lys ¹⁰ H ^ξ	3.34	4.58	4.504	
<i>N</i> -Me-Trp ⁹ H ^{Me}	<i>N</i> -Me-Lys ¹⁰ H ^δ	3.63	5.59	5.450	
<i>N</i> -Me-Trp ⁹ H ^{Me}	<i>N</i> -Me-Lys ¹⁰ H ^γ	2.85	4.04	3.964	
<i>N</i> -Me-Trp ⁹ H ^{Me}	<i>N</i> -Me-Lys ¹⁰ H ^γ	2.85	4.04	3.057	
<i>N</i> -Me-Trp ⁹ H ^α	<i>N</i> -Me-Lys ¹⁰ H ^α	3.78	4.62	4.620	
<i>N</i> -Me-Trp ⁹ H ^α	Amide ¹¹ H ^N	3.95	5.52	5.457	
<i>N</i> -Me-Lys ¹⁰ H ^β	<i>N</i> -Me-Lys ¹⁰ H ^{Me}	2.31	4.14	3.617	
<i>N</i> -Me-Lys ¹⁰ H ^δ	<i>N</i> -Me-Lys ¹⁰ H ^α	2.57	3.84	4.258	+0.42
<i>N</i> -Me-Lys ¹⁰ H ^δ	<i>N</i> -Me-Lys ¹⁰ H ^ξ	2.83	4.16	3.447	
<i>N</i> -Me-Lys ¹⁰ H ^δ	<i>N</i> -Me-Lys ¹⁰ H ^β	2.42	4.36	2.532	
<i>N</i> -Me-Lys ¹⁰ H ^δ	<i>N</i> -Me-Lys ¹⁰ H ^{Me}	4.33	5.66	5.053	
<i>N</i> -Me-Lys ¹⁰ H ^δ	<i>N</i> -Me-Lys ¹⁰ H ^{Me}	4.33	5.66	5.731	+0.07
<i>N</i> -Me-Lys ¹⁰ H ^ε	<i>N</i> -Me-Lys ¹⁰ H ^γ	2.99	5.06	3.218	
<i>N</i> -Me-Lys ¹⁰ H ^γ	<i>N</i> -Me-Lys ¹⁰ H ^α	2.57	3.85	2.597	
<i>N</i> -Me-Lys ¹⁰ H ^γ	<i>N</i> -Me-Lys ¹⁰ H ^ξ	2.88	4.22	3.798	
<i>N</i> -Me-Lys ¹⁰ H ^γ	<i>N</i> -Me-Lys ¹⁰ H ^{Me}	2.96	4.87	4.133	
<i>N</i> -Me-Lys ¹⁰ H ^{Me}	<i>N</i> -Me-Lys ¹⁰ H ^α	3.22	4.44	3.897	
<i>N</i> -Me-Lys ¹⁰ H ^α	Amide ¹¹ H ^N	2.87	4.21	3.349	
<i>N</i> -Me-Lys ¹⁰ H ^β	Amide ¹¹ H ^N	2.94	4.99	3.889	
<i>N</i> -Me-Lys ¹⁰ H ^{Me}	Amide ¹¹ H ^N	3.43	5.38	4.116	

^a Violations of upper bounds (positive sign) and of lower bounds (negative sign) are given in the last column (d_{viol}).

higher populations of the $\chi_1 = 60^\circ$ conformation (gauche+) for the L amino acid residues, and of the $\chi_1 = -60^\circ$ conformation (gauche-) for the D-Phe⁷ residue (Table 6). A strong

Table 5. Φ and Ψ Dihedral Angles of the Average Structure from the Restrained MD (rMD) and from the Trajectory of the Unrestrained MD (MD)

Amino acid residue	Φ_{MD} [°]	Φ_{MD} [°]	Ψ_{MD} [°]	Ψ_{MD} [°]
Nle ⁴	-101	-75.5 ± 39.6	109	29.4 ± 82.5
Asp ⁵	71	-89.7 ± 32.7	144	112.7 ± 16.9
<i>N</i> -Me-His ⁶	-98	-102.4 ± 15.7	78	117.4 ± 19.2
D-Phe ⁷	96	75.0 ± 18.8	-126	-116.0 ± 10.1
<i>N</i> -Me-Arg ⁸	-135	-122.9 ± 8.0	80	83.2 ± 9.9
<i>N</i> -Me-Trp ⁹	-120	-136.6 ± 14.0	63	96.0 ± 12.7
<i>N</i> -Me-Lys ¹⁰	-114	-120.7 ± 9.9	0	83.0 ± 63.4

difference between the two $^3J_{\text{H}\alpha\text{-H}\beta}$ coupling constants together with a sum of both of about 15 Hz indicate however a preferred ($\chi_1 = -60^\circ$) conformation for Asp⁵ ($^3J_{\text{H}\alpha\text{-H}\beta\text{proS}} = 10.7$ Hz) and *N*-Me-Trp⁹ ($^3J_{\text{H}\alpha\text{-H}\beta\text{proR}} = 11.1$ Hz), whereas *N*-Me-His⁶ and *N*-Me-Arg⁸ with identical $^3J_{\text{H}\alpha\text{-H}\beta\text{proR}}$ and $^3J_{\text{H}\alpha\text{-H}\beta\text{proS}}$ coupling constants populate the ($\chi_1 = -60^\circ$) and ($\chi_1 = 180^\circ$) conformations. For D-Phe⁷ the difference of the $^3J_{\text{H}\alpha\text{-H}\beta}$ coupling constants is small indicating a less pronounced preference of the $\chi_1 = 60^\circ$ over the $\chi_1 = 180^\circ$ rotamer. For *N*-Me-Lys¹⁰ the $^3J_{\text{H}\alpha\text{-H}\beta}$ coupling constants indicate populations of 70 to 30% for the $\chi_1 = -60^\circ$ and $\chi_1 = 180^\circ$ rotamers or vice versa. It is not clear, which of both is higher populated as the chemical shifts of the two β protons are degenerated. The *N*-Me-Lys¹⁰ H^ξ signal is slightly broadened to a singlet of 18 Hz line width which has weak shoulders (see Supporting Information) but lacks the expected doublet or triplet structure expected from the coupling to the two δ -Protons when the NMR data is processed for signal intensity. Optimization of the line width by Gaussian multiplication of the FID prior to Fourier transformation led to two similar $^3J_{\text{H}\alpha\text{-H}\xi}$ coupling constants of 6.5 to 7.0 Hz. The similar $^3J_{\text{H}\alpha\text{-H}\beta}$ coupling constants indicate an equilibrium of different conformers within the amide bridged Asp⁵ and *N*-Me-Lys¹⁰ side chains. The slightly broadened *N*-Me-Lys¹⁰ H^ξ signal further suggests that the underlying conformers exchange on a time scale slower than the ns regime what prohibits their sampling by MD simulation in explicit water.

Dynamics of the side chains that are not involved in cyclization were further investigated by 30 ns molecular dynamics simulations in explicit water (Figure 5). For analyzing the side chain dynamics based on the structure obtained from the rMD calculation, position restraints were applied on the carbon and nitrogen atoms of the peptide backbone from Asp⁵ C^α to *N*-Me-Lys¹⁰ C^α. Analysis of the MD simulation performed with such position restraints revealed that all χ_1 populations except of the χ_1 populations of *N*-Me-Arg⁸ and of *N*-Me-Lys¹⁰ were well consistent with the $^3J_{\text{H}\alpha\text{-H}\beta}$ coupling constants (Table 6, Figure 5). The strong preference of $\chi_1 = -60^\circ$ for Asp⁵ and for *N*-Me-Trp⁹ as well as the evenly populated $\chi_1 = -60^\circ$ and $\chi_1 = 180^\circ$ rotamers for Nle⁴ and *N*-Me-His⁶ are indicated by $^3J_{\text{H}\alpha\text{-H}\beta}$ coupling constants and well reproduced by the MD simulation. For D-Phe⁷, the preference of the $\chi_1 = 60^\circ$ rotamer with respect to the $\chi_1 = 180^\circ$ rotamer, which is indicated by the $^3J_{\text{H}\alpha\text{-H}\beta}$ coupling constants, is not reflected by the MD trajectory, which suggests similar populations of the two rotamers.

As indicated by the MD simulation, by the ROEs and by the upfield or downfield chemical shifts, hydrophobic clustering is crucial for the different side chain conformations of peptide **28** in aqueous solution. Stacking of the *N*-Me-His⁶ and D-Phe⁷ side chains, that was also reported in other structural investigations of α -MSH analogs is well observed within the MD trajectory

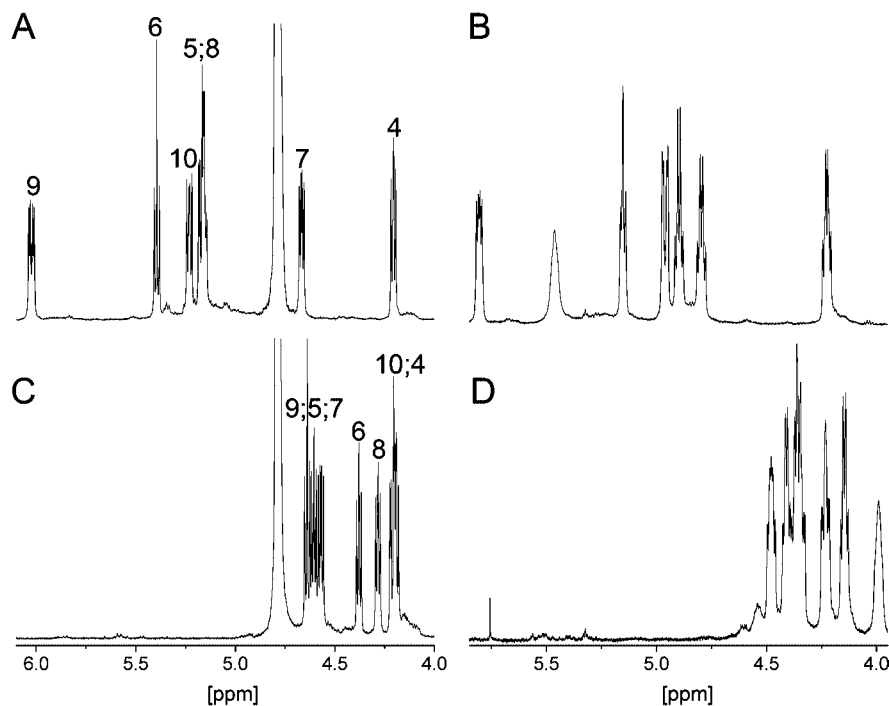


Figure 3. H $^{\alpha}$ regions of ^1H NMR spectra of peptide **28** (A and B) and MT-II (C and D). Spectra A and C were detected in 50 mM sodium acetate- d_4 D $_2$ O buffer (pH 4.5), B and D were detected in DMSO- d_6 . Numbers refer to H $^{\alpha}$ atoms of the respective residues in the α -MSH sequence.

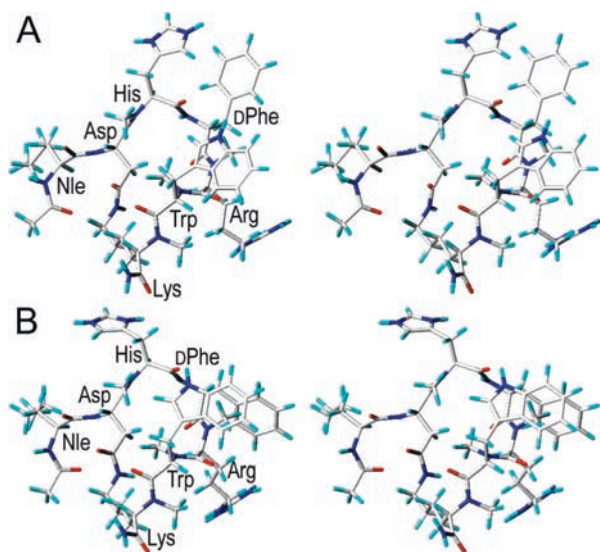


Figure 4. Stereoviews of the solution structure of peptide **28** as determined by NMR spectroscopy and MD calculations. The conformers shown in **A** and **B** possess the same cyclic core structure. The different side chain conformations of *N*-Me-His 6 , *D*-Phe 7 , and *N*-Me-Arg 8 in **A** and **B**, respectively, reflect dynamics in χ dihedral angles observed within the MD.

and is also present in the exemplary conformation shown in Figure 4A. Hydrophobic contacts between the *D*-Phe 7 and *N*-Me-Arg 8 side chains that agree with strong upfield shifts of the *N*-Me-Arg 8 β and γ protons are also observed within the MD trajectory and depicted in the conformation shown in Figure 4B. Overall side chain dynamics as indicated by $^3J_{\text{H}\alpha\text{-H}\beta}$ coupling constants, is reflected by the rotamers shown for *N*-Me-His 6 , *D*-Phe 7 and *N*-Me-Arg 8 in Figure 4A and B, respectively. The clustering of the *N*-Me-Trp 9 indolyl ring with the *N*-methyl group of *N*-Me-Arg 8 , which is observed in Figures 4A and B, is confirmed by ROE contacts between methyl protons and all

Table 6. $^3J_{\text{H}\alpha\text{-H}\beta}$ Coupling Constants as Experimentally Determined from E.COSY a1

	$^3J_{\text{H}\alpha\text{-H}\beta}$ [Hz]		$\rho(\chi_1 = -60^\circ)$ [%]	$\rho(\chi_1 = 180^\circ)$ [%]	$\rho(\chi_1 = 60^\circ)$ [%]
	H $^{\alpha}$ -H $^{\beta}$ proR	H $^{\alpha}$ -H $^{\beta}$ proS			
Nle 4	8.2; 6.2			84	16
Asp 5	3.8	10.7	74	11	15
<i>N</i> -Me-His 6	7.9	7.9	48	48	4
<i>D</i> -Phe 7	5.3	9.2	14	25	61
<i>N</i> -Me-Arg 8	7.0	7.0	40	40	20
<i>N</i> -Me-Trp 9	11.1	4.7	78	19	3
<i>N</i> -Me-Lys 10	9.5, 6			100	0

^a The according χ_1 populations were derived by a linear combination of $^3J_{\text{H}\alpha\text{-H}\beta}(\text{ap}) = 12$ Hz, $^3J_{\text{H}\alpha\text{-H}\beta}(\text{ga}) = 3.5$ Hz.

indolyl protons as well as by a strongly upfield shifted H $^{\text{Me}}$ resonance at 1.559 ppm. ROEs between the *N*-Me-His 6 methyl protons and the *N*-Me-Trp 9 $\delta 1$ and $\epsilon 1$ protons as well as between *D*-Phe 7 H $^{\alpha}$ and *N*-Me-Trp 9 H $^{\epsilon 1}$ are well consistent with the orientation of the indolyl ring given in Figure 4A and B. An additional ROE between the *N*-Me-His 6 methyl protons and the *N*-Me-Trp 9 $\epsilon 3$ proton indicates another orientation of the indolyl group that was not sampled during 30 ns unrestrained MD simulation. In this orientation the indolyl group also seems to stack on top of the *N*-Me-Arg 8 *N*-methyl group as shown in Figure 4 but with the six membered ring of the indolyl group pointing to the left and the five membered ring pointing to the right.

A dispersion of chemical shifts of peptide **28** in DMSO- d_6 (H $^{\alpha}$: 4.245 to 5.824 ppm (Figure 3), H $^{\text{Me}}$: 1.893 to 3.058 ppm), which is similar to the dispersion in the aqueous buffer (H $^{\alpha}$: 4.231 to 6.021 ppm (Figure 3), H $^{\text{Me}}$: 1.559 to 3.115 ppm), indicates that hydrophobic interactions observed in aqueous buffer are also present in the slightly more hydrophobic DMSO. This suggests that such hydrophobic interactions might also be present in hMC1R bound state.

In addition it is often found that stronger conformational preference which is accompanied by stronger biological activity

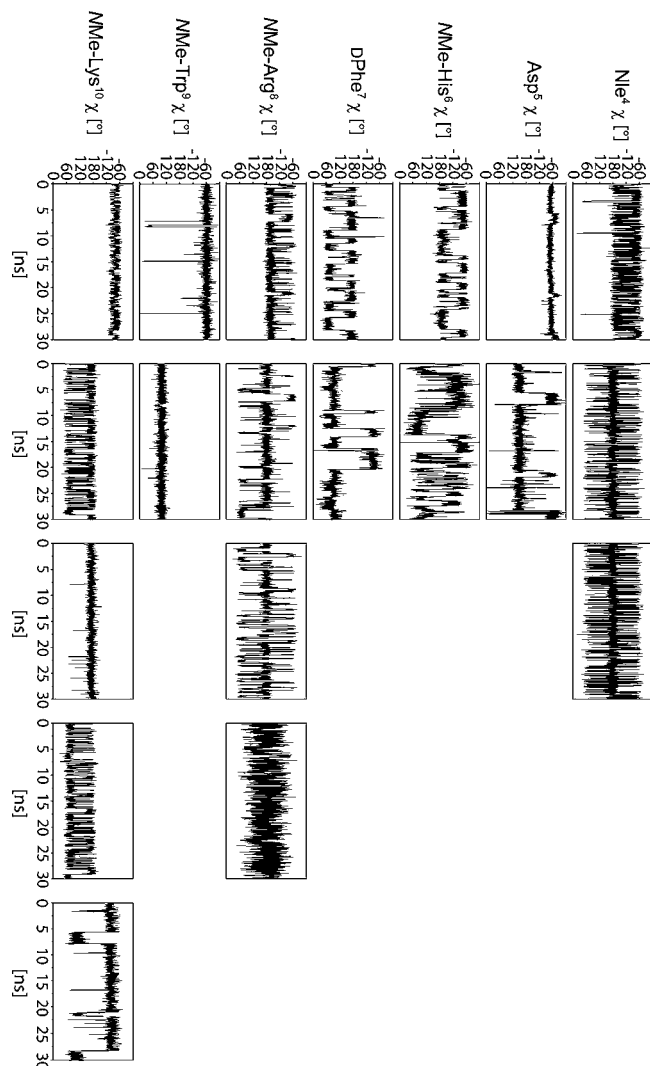


Figure 5. χ dihedral angles as observed during the unrestrained 30 ns MD simulation. The column number (from the left to the right) corresponds to the χ dihedral angle positions within the side chains.

indicates a closer similarity to the bioactive conformation. To our experience these effects seem to be stronger than calculated from populations of conformations. Maybe this can be attributed to the importance of entropic effects in the binding process.

Comparison with Structures of Other Peptidic GPCR Effectors. According to our knowledge, no inverted γ -turn centered at His⁶ has been described so far in structures of similar, but not *N*-methylated α -MSH analogs, like MT-II. β -turns ranging from Asp⁵ to Arg⁸ have more frequently been described than β -turns ranging from His⁶ to Trp⁹ which agrees with the structure of **28** to such a degree as the distance between the Asp⁵ and *N*-Me-Arg⁸ α carbon atoms (6.4 Å) is smaller than the distance between the *N*-Me-His⁶ to *N*-Me-Trp⁹ α carbon atoms (7.6 Å).⁸⁸ In spite of certain similarities with respect to the occurrence of β -turns, the presentation of the side chains of residues *N*-Me-Arg⁸ and *N*-Me-Trp⁹ differs strongly from MT-II. A structure investigation of MT-II suggested that the Arg⁸ side chain is pointing up from the peptide plane and the Trp⁹ side chain is below the peptide plane, when the backbone is oriented as shown in Figure 4.⁸⁸ In contrast, the *N*-Me-Arg⁸

side chain of compound **28** is pointing down from the peptide plane and the *N*-Me-Trp⁹ side chain of compound **28** is pointing up. This provides further evidence that positively charged Arg⁸ is critical for hMC3R and hMC4R binding and functional activities both for the ligand and for the receptor.^{76,89,90} Our earlier chimeric and multiple receptor mutation work demonstrated that the positive charged Arg⁸ plays an important role in binding to the third transmembrane domain using the Asp¹²² and Asp¹²⁶ residues of the hMC3R and hMC4R to achieve binding and functional activities. Multiple *N*-methylation increases the hydrophobicity of the ligand and further reduces the ability of the guanidyl group to interact with the Asp¹²², Asp¹²⁶ to activate the hMCRs,⁷⁶ leading to a loss in the binding and functional activity use. These strong structural differences suggest that the side chain presentation required for MCR activity varies strongly for the individual receptor subtypes. Inherent MT-II flexibility,^{88,89} seems to be high enough for the adaptation to the binding regions of the individual receptor subtypes, whereas **28** possesses a rigid peptide backbone that hinders the pharmacophore of MT-II from interacting properly with the binding pockets of the hMC3R, hMC4R and hMC5R therefore leading to hMC1R selectivity.

Backbone dihedral angles of 96°, -126°, -135° and 80° for D-Phe⁷ Φ , D-Phe⁷ Ψ , *N*-Me-Arg⁸ Φ , and *N*-Me-Arg⁸ Ψ , respectively, resemble type II' β -turn positions *i*+1 and *i*+2. This directed our attention on obvious similarities between peptide **28** and potent somatostatin analogs,^{91–93} which possess a type II' β -turn with an aromatic D amino acid residue in position *i*+1 and a positively charged L amino acid residue in position *i*+2.⁶ Both bind selectively to distinct GPCR subtypes of individual GPCR families (peptide **28** to hMC1R, somatostatin to sst2 and sst5 of the SRIF receptors). Hydrophobic interactions between aromatic side chains stabilize the turn structure of somatostatin analogs, while hydrophobic interactions of the *N*-Me-Trp⁹ methyl group with Asp⁵ and *N*-Me-Lys¹⁰ side chain protons are present in peptide **28**. These similarities in peptide structure and receptor selectivity suggest further similarities between α -MSH analogs and somatostatin analogs with respect to their receptor subtype preference. For somatostatin the empirical correlation of Lys H⁷ upfield shifts with the potency of the ligands have been extensively used to predict activities.⁹³ Possibly, comparable correlations between Arg H⁷ upfield shifts and potency could be found in α -MSH analogs as well.

DG Calculations. DG calculations resulted in a very homogeneous ensemble of compound **28** conformers that were in good agreement with the distance restraints and very similar to the structure shown in Figure 4. The best 30 out of 50 calculated structures possessed an rmsd of 0.27 ± 0.10 Å with respect to the backbone nitrogen and carbon atoms of residues Asp⁵ to *N*-Me-Lys¹⁰. Although ³J coupling constants and broadening of the *N*-Me-Lys¹⁰ H⁵ signal indicated dynamics in the amide linked side chains, the structures obtained from DG possessed

(88) Ying, J.; Kover, K. E.; Gu, X.; Han, G.; Trivedi, D. B.; Kavarana, M. J.; Hruby, V. J. *Biopolymers* **2003**, *71*, 696–716.

(89) Frändberg, P.-A.; Xu, X.; Chhajlani, V. *Biochem. Biophys. Res. Commun.* **1997**, *236*, 489–492.

(90) Grieco, P.; Balse, P. M.; Weinberg, D.; MacNeil, T.; Hruby, V. J. *J. Med. Chem.* **2000**, *43*, 4998–5002.

(91) Veber, D. F.; Holly, F. W.; Paleveda, W. J.; Nutt, R. F.; Bergstrand, S. J.; Torchiana, M.; Glitzer, M. S.; Saperstein, R.; Hirschmann, R. *Proc. Natl. Acad. Sci. U.S.A.* **1978**, *75*, 2636–2640.

(92) Sukopp, M.; Schwab, R.; Marinelli, L.; Biron, E.; Heller, M.; Varkondi, E.; Pap, A.; Novellino, E.; Keri, G.; Kessler, H. *J. Med. Chem.* **2005**, *48*, 2916–2926.

(93) Arison, B. H.; Hirschmann, R.; Veber, D. F. *Bioorg. Chem.* **1978**, *7*, 447–451.

very similar homogeneous *N*-Me-Lys¹⁰ χ_1 and χ_2 dihedral angles ($\chi_1 = -55.2^\circ \pm 2.01^\circ$, $\chi_2 = -109^\circ \pm 3.73^\circ$). The observation of only one preferred χ_1 dihedral angle did not reflect the $^3J_{\text{H}\alpha\text{-H}\beta}$ coupling constants (Table 6) and the only populated eclipsed χ_2 rotamer was thermodynamically unfavorable. Apparently, conformation averaging in the *N*-Me-Lys¹⁰ side chain led to a number of conformation averaged distance restraints that forced the lactam bridged *N*-Me-Lys¹⁰ side chain into conformations during DG calculations that could not be highly populated at equilibrium.

Restrained Molecular Dynamics Calculations. The best DG structure in respect of violations of experimental distance restraints was subjected to refinement by restrained molecular dynamics (rMD) calculation in explicit water. The average structure of the rMD calculation was very similar to the DG starting structure (rmsd = 0.69 Å with respect to backbone heavy atoms from Asp⁵ to *N*-Me-Lys¹⁰). Within the cyclic core structure significant changes occurred only in the *N*-Me-Lys¹⁰ side chain, that was strained in the starting conformer as side chain dihedral angles were eclipsed ($\chi_2 = -111^\circ$ and $\chi_3 = -137^\circ$). As expected, the force field applied during restrained MD calculation rotated the dihedral angles within the *N*-Me-Lys¹⁰ side chain to thermodynamically feasible values ($\chi_2 = -169^\circ$ and $\chi_3 = 163^\circ$).

Unrestrained Molecular Dynamics Calculations. The average structure obtained from the rMD calculation was further refined by extended (30 ns) unrestrained MD simulation in explicit water. This led to significant changes of some backbone dihedral angles (Table 5) that were accompanied by further conformational changes in the lactam bridged *N*-Me-Lys¹⁰ side chain. The changes of backbone dihedral angles led to significant violations of distance restraints and most $^3J_{\text{H}\alpha\text{-H}\beta}$ coupling constants were not consistent with the χ_1 populations extracted from the MD trajectory. Consistency with $^3J_{\text{H}\alpha\text{-H}\beta}$ coupling constants and with distance restraints was much higher in a trajectory of an MD simulation in which the conformation of the peptide backbone obtained from rMD was conserved by applying position restraints on all backbone carbon and nitrogen atoms from Asp⁵ C α to *N*-Me-Lys¹⁰ C α .

We believe that the artificial strains in the lactam bridged side chains, that were described above, induced the conformational changes that were observed in the peptide backbone during 30 ns non position restrained MD simulation. The slight variations in Φ and Ψ dihedral angles seemed to be energetically less demanding than flips between individual staggered conformations within the *N*-Me-Lys¹⁰ side chain. Apparently, the backbone compensated for the strains within the lactam bridged side chains during the unrestrained MD simulation and position restraining of the backbone during the unrestrained MD simulation seems to be a legitimate way to avoid faulty changes of backbone dihedral angles.

Conclusions

Multiple *N*-methylation in MT-II led to several derivatives in which the affinity and activity for hMC1R could be retained, but simultaneously the binding affinity to the other 3 melanocortin receptors was completely lost. Hence, selectivity and retained activity was achieved in this way. A careful analysis of the conformation of the most active (13 nM) compound reveals a strong preference of one backbone conformation, which indicates a strongly reduced conformational space in comparison to the nonmethylated MT-II. Hence, this work again shows that restriction of peptide backbone conformation resulted

in strong receptor subtype selectivity with retained or even improved activity for an individual receptor subtype. This approach, discussed by us already a quarter of a century ago^{94,95} is not achievable only by cyclization but can be further increased by multiple *N*-methylation.⁴⁸ With an increasing extent of introduction of *N*-methyl groups into its backbone, MT-II derivatives lose their ability to bind to particular hMCRs out of the total family of melanocortin receptors. This leads in two cases (peptides **24** and **28**) to highly selective and potent agonists for the hMC1R, but also to antagonists and compounds with both, agonist and antagonist activities. These compounds possess multiple amide bonds that are *N*-methylated which was recently reported to be a possible key toward bioavailability⁵ and maybe also enhanced oral bioavailability⁶ of peptides. Whereas the effect of *N*-methylation on receptor subtype selectivity is strongly supported by our results, the effect on pharmacological properties that have been improved in other examples⁴⁻⁶ has to be demonstrated for the *N*-methylated MT-II derivatives. These investigations are in progress.

Experimental Section

Materials. *N* α -Fmoc-amino acids, peptide coupling reagents, Rink amide MBHA resin and solvents were reagent grade and used without further purification unless otherwise noted. These chemicals were obtained from Aldrich, Novabiochem, Iris Biotech GmbH, Merck, NeoMPS, ORPEGEN Pharma and GLS. The following amino acids were used: Fmoc-Lys(Alloc)-OH, Fmoc-Trp(Boc)-OH, Fmoc-Arg(Pbf)-OH, Fmoc-D-Phe-OH, Fmoc-His(Trt)-OH, Fmoc-Asp(OAllyl)-OH and Fmoc-Nle-OH. The polypropylene reaction vessels (syringes with frits) were purchased from B. Braun Melsungen AG. The purity of the peptides was checked by analytical reverse-phase HPLC using an Amersham Pharmacia Biotech Äkta Basic 10F with a ODS-A C18 (120 Å, 5 μm , 250 mm \times 4.6 mm) column (Omniscrom YMC Europe GmbH) monitored at 220 and 254 nm and by high resolution mass spectral analysis.

Synthesis. The MT-II analogues were synthesized manually by the Fmoc-SPPS using methods described in refs 96 and 97.

Rink amide MBHA resin (0.3 g, 4-(2',4'-dimethoxyphenyl)-Fmoc-aminomethyl)-phenoxyacetamido-norleucyl-MBHA resin) in a 10 mL syringe with a frit on the bottom was swollen in NMP (3 mL) for 10 min. The Fmoc protecting group on the Rink linker was removed by 20% piperidine in NMP (1 \times 8 min, 1 \times 12 min). The resin was washed with NMP (5 \times 3 mL). The first *N* α -Fmoc-amino acid was coupled using preactivated ester (3 equiv *N* α -Fmoc-amino acid, 3 equiv TBTU, 3 equiv HOBt and 8 equiv DIEA) in NMP. The coupling mixture was transferred into the syringe with the resin and shaken for 3 h. Afterward the resin was washed with NMP (5 \times 3 mL). Complete coupling was confirmed by HPLC monitoring. Therefore the resin was washed with DCM (2 \times 3 mL). A small amount of resin was taken out of the syringe and three drops of a mixture of trifluoroacetic acid/triethylsilane/water (95:2.5:2.5, v/v/v) was added. After 10 min, acetonitrile and water were added, and after filtration, HPLC and ESI-MS showed complete coupling. The peptide sequences were continued by consecutively coupling of the particular amino acids. *N*-Methylation was carried out after coupling of the corresponding amino acid. This procedure includes three steps. First, the *N*-terminal *N* α -Fmoc-deprotected amino acid was protected as an *N* α -*o*-nitrobenzene sulfonamide by reaction with 5 equiv of *o*-nitrobenzenesulfonyl chloride (*o*-NBS) and 10 equiv of collidine in NMP (15 min). The

(94) Kessler, H. *Angew. Chem., Int. Ed.* **1982**, *21*, 512–523.

(95) Hruby, V. J. *Life Sci.* **1982**, *31*, 189–199.

(96) Mayorov, A. V.; Han, S. Y.; Cai, M.; Hammer, M. R.; Trivedi, D.; Hruby, V. J. *Chem. Biol. Drug. Des.* **2006**, *67*, 329–335.

(97) Heckmann, D.; Kessler, H. *Methods Enzymol.* **2007**, *426*, 463–503.

methylation was done under Mitsunobu conditions⁹⁸ with 5 equiv of triphenylphosphine, 10 equiv of methanol and 5 equiv of diisopropyl azodicarboxylate (DIAD) in THF (10 min). Then the *o*-NBS group was removed with 10 equiv of 2-mercaptoethanol and 5 equiv of DBU in NMP (5 min). This deprotection procedure was repeated once. For the coupling of the next amino acid, 3 equiv HATU, 3 equiv HOAt and 8 equiv DIEA were used. After coupling of the last amino acid Fmoc-Nle-OH and Fmoc deprotection as described above, acetylation was achieved by treatment of the DCM washed resin (3 × 3 mL) with acetic anhydride/DCM/DIEA (25:75:2.5, v/v/v, 3 mL) for 30 min and washing of the resin with DCM (5 × 3 mL). The next step was the removal of the *N*^ε-Alloc group of Lys and the β-allyl group of Asp.^{96,97,99} For this, a solution of PhSiH₃ (24 equiv) in 1 mL DCM was added to the peptide resins. Then a solution of Pd(PPh₃)₄ (0.25 equiv) in 2 mL DCM was added and the reaction allowed to proceed for 30 min. The peptide resins were washed with DCM (3 × 3 mL), NMP (2 × 3 mL), afterward twice with 0.5% DIEA in DMF (v/v) and 0.5% sodium diethyldithiocarbamate trihydrate (DEDTC) in DMF (w/w) to remove any remaining traces of the Pd catalyst,¹⁰⁰ followed by NMP (5 × 3 mL). The macrocyclic lactam ring formation was then mediated by addition of TBTU (3 equiv), HOBt (3 equiv) and DIEA (8 equiv) for 3 h. The cyclized peptides were cleaved off solid support using 3 mL trifluoroacetic acid/triethylsilane/water (95:2.5:2.5, v/v/v, 1 × 3 h, 1 × 15 min), and the crude peptides were precipitated by dropping the solution in chilled diethyl ether to give white to light yellow precipitates. The resulting peptide suspensions were centrifuged for 5 min at 4000 rpm, and the liquid was decanted. The crude peptides were washed with chilled diethyl ether (2 × 30 mL), and after the final centrifugation, dried under vacuum overnight. Purification was performed by HPLC using a ODS-A C18 (120 Å, 5 μm, 250 mm × 20 mm) column (Omniscrom YMC Europe GmbH) eluting with a linear gradient of acetonitrile and water containing 0.1% TFA. The products were obtained by lyophilization of the appropriate fractions after removal of the acetonitrile by rotary evaporation. Analysis by analytical HPLC and HPLC-MS (Supporting Information) showed the peptides to be pure (>95%). The purified peptides were isolated in 2–14% overall yields.

Biological Activity Assays

Receptor Binding Assay. Competition binding experiments were carried out using whole HEK293 cells stably expressing human MC1, MC3, MC4, and MC5 receptors as described before.^{101–103} HEK293 cells transfected with hMCRs^{101–103} were seeded on 96-well plates 48 h before assay (50,000 cells/well). For the assay, the cell culture medium was aspirated and the cells were washed once with a freshly prepared MEM buffer containing 100% minimum essential medium with Earle's salt (MEM, GIBCO), and 25 mM sodium bicarbonate. Next, the cells were incubated for 40 min at 37 °C with different concentrations of unlabeled peptide and labeled [¹²⁵I]-[Nle⁴,D-Phe⁷]-α-MSH (Perkin-Elmer Life Science, 20 000 cpm/well, 33.06 pM) diluted in a 125 μL of freshly prepared binding buffer containing 100% MEM, 25 mM HEPES (pH 7.4), 0.2% bovine serum albumin, 1 mM 1,10-phenanthroline, 0.5 mg/L leupeptin,

200 mg/L bacitracin. The assay medium was subsequently removed, the cells were washed once with basic medium, and then lysed by the addition of 100 μL of 0.1 M NaOH and 100 μL of 1% Triton X-100. The lysed cells were transferred to 12 × 75 mm borosilicate glass tubes, and the radioactivity was measured by a Wallac 1470 WIZARD Gamma Counter. The results are shown in Table 1.

Adenylate Cyclase Assay. HEK 293 cells transfected with human melanocortin receptors¹⁰³ were grown to confluence in MEM medium (GIBCO) containing 10% fetal bovine serum, 100 units/mL penicillin and streptomycin, and 1 mM sodium pyruvate. The cells were seeded on 96-well plates 48 h before assay (50 000 cells/well). For the assay, the cell culture medium was removed and the cells were rinsed with 100 μL of MEM buffer (GIBCO). An aliquot (100 μL) of the Earle's balanced salt solution with 5 nM isobutylmethylxanthine (IBMX) was placed in each well along for 1 min at 37 °C. Next, aliquots (25 μL) of melanotropin peptides of varying concentration were added, and the cells were incubated for 3 min at 37 °C. The reaction was stopped by aspirating the assay buffer and adding 60 μL ice-cold Tris/EDTA buffer to each well, then placing the plates in a boiling water bath for 7 min. The cell lysates were then centrifuged for 10 min at 2,300g. A 50 μL aliquot of the supernatant was transferred to another 96-well plate and placed with 50 μL [³H] cAMP and 100 μL protein kinase A (PKA) buffer in an ice bath for 2–3 h. The PKA buffer consisted of Tris/EDTA buffer with 60 μg/mL PKA and 0.1% bovine serum albumin by weight. The incubation mixture was filtered through 1.0 μm glass fiber filters in MultiScreen-FB 96-well plates (Millipore, Billerica, MA). The total [³H] cAMP was measured by a Wallac MicroBeta TriLux 1450 LSC and Luminescence Counter (PerkinElmer Life Science, Boston, MA). The cAMP accumulation data for each peptide analogue was determined with the help of a cAMP standard curve generated by the same method as described above. IC₅₀ and EC₅₀ values represent the mean of two experiments performed in triplicate. IC₅₀ and EC₅₀ estimates and their associated standard errors were determined by fitting the data using a nonlinear least-squares analysis, with the help of GraphPad Prism 4 (GraphPad Software, San Diego, CA). The maximal cAMP produced at 10 μM concentration of each ligand was compared to the amount of cAMP produced at 10 μM concentration of the standard agonist MT-II, and is expressed in percent (as % max effect) in the Table 2. The antagonist properties of the lead compounds were evaluated by their ability to competitively displace the MT-II agonist in a dose-dependent manner, at up to 10 μM.

Data Analysis. IC₅₀ and EC₅₀ values represent the mean of two experiments performed in triplicate. IC₅₀ and EC₅₀ estimates and their associated standard errors were determined by fitting the data using a nonlinear least-squares analysis, with the help of GraphPad Prism 4 (GraphPad Software, San Diego, CA).

NMR Spectroscopy. DQF-COSY, E.COSY, TOCSY, ROE-SY, ¹³C-HMBC and ¹³C-HSQC spectra were recorded at 298 K on a Bruker DMX spectrometer operating at 600 MHz. A COLOC spectrum¹⁰⁴ was recorded at 298 K on a Bruker Avance III spectrometer operating at 600 MHz. A phase sensitive HMBC and a reference HSQC spectrum with offset and rf-amplitude-compensated BEBOP^{105,106} and BIBOP pulses^{107,108}

(98) Mitsunobu, O. *Synthesis* **1981**, 1, 1–28.

(99) Thieriet, N.; Alsina, J.; Giralt, E.; Guibe, F.; Albericio, F. *Tetrahedron Lett.* **1997**, 38, 7275–7278.

(100) Mayorov, A. V.; Cai, M.; Chandler, K. B.; Petrov, R. R.; VanScoy, A. R.; Yu, Z.; Tanaka, D. K.; Trivedi, D.; Hruby, V. J. *J. Med. Chem.* **2006**, 49, 1946–1952.

(101) Cai, M.; Mayorov, A. V.; Ying, J.; Stankova, M.; Trivedi, D.; Cabello, C.; Hruby, V. J. *Peptides* **2005**, 26, 1481–1485.

(102) Cai, M.; Mayorov, A. V.; Cabello, C.; Stankova, M.; Trivedi, D.; Hruby, V. J. *J. Med. Chem.* **2005**, 48, 1839–1848.

(103) Cai, M.; Cai, C.; Mayorov, A. V.; Xiong, C.; Cabello, C. M.; Soloshonok, V. A.; Swift, J. R.; Trivedi, D.; Hruby, V. J. *J. Pept. Res.* **2004**, 63, 116–131.

(104) Kessler, H.; Griesinger, C.; Zarbock, J.; Loosli, H.-R. *J. Magn. Reson.* **1984**, 57, 331–336.

(105) Skinner, T. E.; Reiss, T. O.; Luy, B.; Khaneja, N.; Glaser, S. J. J. *Magn. Reson.* **2003**, 163, 8–15.

were detected at 298K on a Bruker Avance III spectrometer operating at 750 MHz.^{109,110} Samples were prepared in 50 mM Sodium acetate-d₄ buffer (pH 4.5, 10% D₂O, 0.05% NaN₃) at concentrations of 12–38 mM. This low pH was chosen to keep hydrogen exchange induced line broadening small and to enhance comparability with numerous earlier structural studies on MCR effectors that were performed under the same conditions. Sodium 3-(trimethylsilyl)propionate-2,2,3,3-d₄ (¹H at 0.000 ppm) was used as internal standard. Data were processed with Topspin 1.3 software from Bruker. The homo- and heteronuclear experiments DQF-COSY, E.COSY, TOCSY, ROESY, and magnitude mode ¹³C-HMBC were performed with a spectral width of 11 ppm for ¹H and 180 ppm for ¹³C. Individual HSQC spectra covering aliphatic (¹³C offset = 35 ppm, spectral width = 50 ppm) and aromatic ¹³C resonances (¹³C offset = 120 ppm, spectral width = 30 ppm) were detected. The phase sensitive HMBC spectrum and the reference HSQC spectrum were detected with a spectral width of 9 ppm for ¹H and 190 ppm for ¹³C. A COLOC spectrum was detected with spectral widths of 9.5 ppm for ¹H and 190 ppm for ¹³C. The increments in t₁ and t₂ were adjusted to the information extracted from the individual experiments, ranging from 384 to 2048 increments in t₁ and from 4096 to 16 384 complex data points in t₂. Depending on the sample concentration and the individual experiments, 16 to 48 transients were averaged for each t₁ value. A mixing time of 80 ms was used for TOCSY (spin lock field: 6 kHz; mixing sequence MLEV-17). Water signal suppression was achieved by WATERGATE techniques.¹¹¹ The sequential assignment was obtained from heteronuclear J correlations that were extracted from HSQC and HMBC spectra. A compensated ROESY experiment, which was used for the extraction of inter proton distances, was performed with 150 ms mixing time and a spin lock field of 4000 kHz.¹¹² The volume integrals of the individually assigned cross-peaks were compensated for offset effects and converted into distance constraints using the isolated spin pair approximation.¹¹³ To compensate for watergate solvent signal suppression artifacts, of any two cross peaks representing an internuclear distance, the peak with the higher water resonance offset in the direct dimension was preferably considered for distance calculations. The ROESY cross-peak volumes were calibrated against the distance (1.78 Å) between the prochiral *N*-Me-Lys¹⁰ H^ε protons. Upper and lower distance limits were set to plus and minus 10% of the calculated distances, respectively. For distance restraints referring to nonstereospecifically assigned methylene protons, another 0.7 Å was added on upper bounds as pseudoatoms and multiplicity corrections. For distance restraints referring to methyl protons, subtraction of 10% for the lower bounds was omitted and another 0.9 Å was added on upper bounds as pseudoatoms and multiplicity corrections. 18 intraresidual, 36 sequential interresidual and 9 nonsequential interresidual ROE

derived distance restraints were used for structure calculations, with restraints between the lactam bridged residues Asp⁵ and *N*-Me-Lys¹⁰ counted as sequential.

³J_{HN-Hα} coupling constants were determined from 1D ¹H NMR spectra, ³J_{HO-Hβ} coupling constants from E.COSY and heteronuclear ³J_{C-H} coupling constants from HMBC and reference HSQC spectra.^{109,110,114,115}

Structure Calculations for 28. The structural NMR refinement protocol included distance geometry (DG) calculations, energy minimizations, and molecular dynamics (MD) simulations. The DG program DISGEO was used to generate structures consistent with the 63 distance restraints derived from the ROEs.^{116,117} The DG procedure started with the embedding of 50 structures using random metrization. The structures obtained from DG were evaluated according to the lowest total restraint violations and additionally counterchecked for close contacts of protons that did not show corresponding ROESY crosspeaks. Among 30 structures that were in best accordance with experimentally derived restraints, all had identical peptide backbone conformations.

Restrainted MD calculations (rMD) were carried out employing the module DISCOVER of the INSIGHT II 2001 program (Biosym/MSI Inc.) with the CVFF force field. The ROE restraints were included with a force constant of 10 kcal mol⁻¹ Å⁻². The calculations were done with the explicit-image model of periodic boundary conditions. The best structure resulting from the DG calculation was placed in a cubic box of length 30 Å and soaked with water. After energy minimization using steepest descent and conjugate gradient, the system was heated gradually starting from 10 K and increasing to 50, 100, 150, 200, 250 and 300 K in 1 ps steps, each by direct scaling of velocities. The system was equilibrated for 50 ps with temperature bath coupling. Coordinates were saved every 100 fs for another 150 ps. The average structure of the 150 ps rMD calculation was subjected to energy minimization and further investigated by unrestrained MD simulations.

The GROMACS 4.0 software package (www.gromacs.org)^{118–120} was used to perform unrestrained MD calculations. Visualization of the simulation trajectories was performed using the software packages VMD¹²¹ and SYBYL 8.0.¹²² The scripts *g_cluster*, *g_dist* and *g_angle*, that were used for analysis of the MD trajectory, were all packaged with GROMACS. The 53a6 united atom (CH, CH₂ and CH₃ groups represented as a single atom) forcefield, one of the GROMOS96 force fields,¹²³ was used for the molecular dynamic simulations. Rigid SPC water which was constrained using SETTLE¹²⁴ served as water model. Solute bonds were constrained by the SHAKE algo-

- (106) Skinner, T. E.; Reiss, T. O.; Luy, B.; Khaneja, N.; Glaser, S. J. *J. Magn. Reson.* **2004**, *167*, 68–74.
 (107) Kobzar, K.; Skinner, T. E.; Khaneja, N.; Glaser, S. J.; Luy, B. *J. Magn. Reson.* **2004**, *170*, 236–243.
 (108) Luy, B.; Kobzar, K.; Skinner, T. E.; Khaneja, N.; Glaser, S. J. *J. Magn. Reson.* **2005**, *176*, 179–186.
 (109) Verdier, L.; Sakhaii, P.; Zweckstetter, M.; Griesinger, C. *J. Magn. Reson.* **2003**, *163*, 353–359.
 (110) Kobzar, K.; Luy, B. *J. Magn. Reson.* **2007**, *186*, 131–141.
 (111) Piotto, M.; Saudek, V.; Sklenár, V. *J. Biomol. NMR* **1992**, *2*, 661–665.
 (112) Griesinger, C.; Ernst, R. *J. Magn. Reson.* **1987**, *75*, 261–271.
 (113) Kumar, A.; Wagner, G.; Ernst, R.; Wuthrich, K. *J. Am. Chem. Soc.* **1981**, *103*, 3654–3658.

- (114) Eberstadt, M.; Gemmecker, G.; Mierke, D. F.; Kessler, H. *Angew. Chem., Int. Ed.* **1995**, *34*, 1671–1695.
 (115) Richardson, J. M.; Titman, J. J.; Keeler, J.; Neuhaus, D. *J. Magn. Reson.* **1991**, *93*, 533–553.
 (116) Mierke, D. F.; Kessler, H. *Biopolymers* **1993**, *33*, 1003–1017.
 (117) Havel, T. F. *Prog. Biophys. Mol. Biol.* **1991**, *56*, 43–78.
 (118) Lindahl, E.; Hess, B.; van der Spoel, D. *J. Mol. Model.* **2001**, *7*, 306–317.
 (119) van der Spoel, D.; Lindahl, E.; Hess, B.; Groenhof, G.; Mark, A. E.; Berendsen, H. J. C. *J. Comput. Chem.* **2005**, *26*, 1701–1718.
 (120) van der Spoel, D.; Lindahl, E.; Hess, B.; van Buuren, A. R.; Apol, P. J.; Meulenhoff, P. J.; Tieleman, D. P.; Sijbers, A. L. T. M.; Feenstra, K. A.; van Drunen, R.; Berendsen, H. J. C. *Gromacs User Manual version 4.0*, 2005; <http://www.gromacs.org>.
 (121) Humphrey, W.; Dalke, A.; Schulten, K. *J. Mol. Graph.* **1996**, *14* (33–38), 27–38.
 (122) SYBYL 7.3; Tripos International: St. Louis, MO, 2006.

rithm¹²⁵ and temperature and pressure control was executed by Berendsen coupling.¹²⁶ Periodic boundary conditions were employed on a octahedral simulation box, which was built with a distance of 1.4 nm for the solute. Cut off distances of 1.4 nm for electrostatic and Lennard-Jones nonbonding interactions were applied. Simulation time steps were set to 2 fs. Upon addition of two acetate counterions and soaking of the box with water, the system was equilibrated by an initial minimization and subsequent 50 ps MD simulations at 50, 100, 150, 200, 250, and 298 K using position restraints. Within the individual MD steps, the temperature was gradually increased, while the force constants of the position restraints were decreased exponentially from 250 000 KJmol⁻¹nm⁻² at 50 K to 25 KJmol⁻¹nm⁻² at 250 K. At 298 K no position restraints were applied. For adjacent pressure equilibration a 100 ps MD simulation was performed

- (123) van Gunsteren, W. F.; Billeter, S. R.; Eising, A. A.; Hunenberger, P. H.; Krueger, P.; Mark, A. E.; Scott, W. R. P.; Tironi, I. G. in *Biomolecular simulation: the GROMOS96 manual and user guide*, 1st ed., Hochschulverlag AG an der ETH Zürich, Zürich, 1996.
- (124) Miyamoto, S.; Kollman, P. A. *J. Comput. Chem.* **1992**, *13*, 952–962.
- (125) Ryckaert, J. P.; Ciccotti, G.; Berendsen, H. J. C. *J. Comput. Phys.* **1977**, *23*, 327–341.
- (126) Berendsen, H. J. C.; Postma, J. P. M.; van Gunsteren, W. F.; Dinola, A.; Haak, J. R. *J. Chem. Phys.* **1984**, *81*, 3684–3690.

at 298 K. The final 30 ns MD simulation was carried out at 298 K. Coordinates were saved every 10 ps. For the MD simulation with strict conservation of the peptide backbone obtained from the restrained MD simulation, position restraints of 250 000 KJmol⁻¹nm⁻² were applied on all backbone carbon and nitrogen atoms between Asp⁵ C^α and N-Me-Lys¹⁰ C^α.

Acknowledgment. These studies were supported in parts by grants from the U.S. Public Health Service, National Institutes of Health, DK017420 and DA06284. We also thank the Humboldt Foundation for the support via the Max-Planck Award, the Deutschen Forschungsgemeinschaft (DFG) for financial support and Prof. Eberle in Basel for initial measurements of activities. J.G.B. thanks Oliver Demmer for help with GROMACS and Dr. Burkhard Luy for help with HMBC and reference HSQC spectra.

Supporting Information Available: Table listing sequences and physicochemical properties of the *N*-methylated MT-II analogs, HPLC chromatograms, ¹H NMR spectra, and f2 slice of the ROESY crosspeak between *N*-Me-Lys¹⁰ H^ζ and Asp⁵ H^β_{proS}. This material is available free of charge via the Internet at <http://pubs.acs.org>.

JA101428M